Investigation of Interactions of TiO$_2$ Nanoparticles with Dissolved Components of Surface Waters under Natural Conditions

by

Narjes Tayyebi Sabet Khomami

From Tehran, Iran

Accepted Dissertation thesis for the partial fulfillment of the requirements for

a Doctor of Natural Sciences

Fachbereich 7: Natur- und Umweltwissenschaften

Rheinland-Pfälzische Technische Universität (RPTU)

Kaiserslautern-Landau

Thesis examiners:
Prof. Dr. Gabriele E. Schaumann, RPTU
Dr. Allan Philippe, RPTU

Date of oral examination:
27.10.2023

Declaration

I declare that this Ph.D. thesis, entitled "Investigation of Interactions of TiO_2 Nanoparticles with Dissolved Components of Surface Waters under Natural Conditions" was prepared and carried out on my own. All assistance, contributors, and authors are declared and indicated in this thesis. This thesis has never been submitted elsewhere for an exam, neither to any other university nor scientific institution.

Landau in der Pfalz, 14.11.2023   Narjes Tayyebi

Place, date   **Signature**

Published parts of the thesis

This Ph.D. thesis consists of eight chapters that represent three published research papers. The experiments were conducted at the Institute for Environmental Sciences (iES-Landau), Rheinland-Pfälzische Technische Universität (RPTU), Campus Landau.

Chapter 3 was published in Environmental Science Nano (2020):

Tayyebi, N., Philippe, A., Abu Quba, A.A. Lechtenfeld, O. J., Guigner, J. M., Heissler, S., & Schaumann, G. E. (2020). Validation of a field deployable reactor for in-situ formation of NOM-engineered nanoparticle corona. Environmental Science: Nano, 7(2), 486-500.

N. Tayyebi and Dr. Philippe designed the concept. N. Tayyebi did the methodology, validation, investigation (laboratory and field work), writing original draft as well as reviewing and editing of the final manuscript, and presentation of the final work under the supervision of Prof. Dr. Schaumann and Dr. Philippe. Abd Alaziz Abu Quba, Oliver J. Lechtenfeld, Jean-Michel Guigner, and Stefan Heissler did the AFM, FT-ICR MS, HR-TEM, and ATR-FTIR analyses, respectively, and helped with the corresponding interpretations. Prof. Dr. Schaumann was in charge of the conception and discussion of the interpretations as long as project administration and funding acquisition. All the coauthors contributed to the review and editing of the final manuscript.

Chapter 4 was published in Environmental Science Nano (2021):

Tayyebi , N., Patel, P. M., Jusi, C. P., Trouillet, V., David, J., Schaumann, G. E., & Philippe, A. (2021). Influential parameters of surface waters on the formation of coating on TiO_2 nanoparticles under natural conditions. Environmental Science: Nano, 8(11), 3153-3166.

N. Tayyebi did the conceptualization, methodology, software, formal analysis, validation, investigation (laboratory and field work), writing of the original draft as well as reviewing and editing, and presentation of the final work under the supervision of Dr. Philippe. Parthvi Mayurbhai Patel, and Cynthia Precious Jusi, helped with the investigation part, as a part of their master theses, under the supervision of Dr. Philippe and N. Tayyebi. Dr. Philippe and N. Tayyebi carried out 2D IR measurements. Vanessa Trouillet, and Jan David did the XPS and TGA analyses, respectively, and helped with the corresponding interpretations. Dr. Philippe was involved in data analysis. Prof. Dr. Schaumann was in charge of the conception and discussion

of the interpretations as long as project administration and funding acquisition. All the coauthors contributed to the review and editing of the final manuscript.

Chapter 5 was published in Coatings (2022):

Tayyebi, N., Welle, A., Kunz, S., & Philippe, A. (2022). Sorption of Fulvic Acids onto Titanium Dioxide Nanoparticles Extracted from Commercial Sunscreens: ToF-SIMS and High-Dimensional Data Analysis. Coatings, 12(3), 335.

N. Tayyebi, and Dr. Philippe designed the concept and did the methodology, and validation. N. Tayyebi did the investigation, and writing original draft as well as reviewing and editing, and presentation of the final work under the supervision of Dr. A. Philippe. Stefan Kunz and Dr. Philippe wrote the acquired codes for the R program. ToF-SIMS analysis and the corresponding interpretations were performed by Dr. A. Welle. All the coauthors contributed to the review and editing of the final manuscript.

برای پدرم و تشویق هایش

Acknowledgments

Contents

Abstract

The booming global market of nanomaterials in the last few decades has led to the inevitable emission of these materials into aquatic environments; hence, understanding their physical, chemical, and biological transformations has become a big concern for environmental scientists. Despite a great deal of effort made to understand the mobility, fate, and risk assessment of e.g, TiO_2 nanoparticles, it is still unclear if the obtained results, under lab-controlled conditions, can be generalized to realistic released nanoparticles in aquatic environments since the complex dynamics of environmental conditions are not completely reproducible under controlled conditions.

In the present study, we proposed a new approach to expose TiO_2 nanoparticles to environmental conditions of natural surface waters by making use of dialysis membranes as passive reactors. The function of these reactors is based on the permeability of the membrane to the dissolved matter of surface waters while TiO_2 nanoparticles do not pass through the membrane. These systems benefit from the fact that although the complexity and temporal variability of most of the environmental parameters of surface waters are reproducible inside the reactors, colloidal and particulate interferences remain separated. Furthermore, no significant reduction in pore size i.e., membrane fouling is observed in dialysis bags after exposure to surface waters which validates the efficiency of the system.

Taking advantage of these reactors to expose nanoparticles to surface waters, we investigated the influential physicochemical parameters of the surface waters on the formation of natural coating onto nanoparticles. Hence, dialysis bags were used to expose TiO_2 nanoparticles, in situ, to ten different surface waters in the spring and summer of 2019. Due to the complexity of the natural dissolved matter of the surface waters as long as their low natural concentrations, we needed to use a combination of analytical techniques and multivariate data analysis to investigate the coatings. The initial findings were similar to the lab-controlled exposure studies in the literature showing pH, electrical conductivity, and Ca^{2+}- Mg^{2+} concentration as the three most important parameters of surface waters controlling the formation of coatings. Nonetheless, we came across a phenomenon being overlooked under lab-controlled conditions; natural coatings are composed of not only organics (DOM: dissolved organic matter) but also inorganics (carbonate) which implies that their realistic coatings are more complex than what the previous studies described.

The second part of this thesis focused on investigating the interactions of more realistic nanoparticles (extracted TiO_2 nanoparticles from 11 sunscreens) with DOM. Using ToF-SIMS combined with high-dimensional data analysis, we tried to find a general DOM-sorption pattern among TiO_2 nanoparticles since finding this pattern could have ultimately opened a way to assess the fate of (more) realistic nanoparticles in aquatic environments. Contrary to our expectations, the results showed a unique sorption pattern for each sunscreen controlled by the composition of the sunscreens implying that the sorption pattern of each sunscreen should be investigated individually. In the next step of this study, we used random forest to extract the most important fragments of DOM sorbed onto each sunscreen followed by an effort to assign these important masses to chemical fragments.

Trying to provide a comprehensive understanding of interactions of the released n-TiO_2 in aquatic environments, in future studies, we are going to expand our coating research to different types of TiO_2 nanoparticles, such as extracted particles from paint, where the reaction media (surface waters) are covering a wide range of water parameters representative of various ecosystems. Making use of state-of-the-art techniques as long as multivariate data analysis, we will try to achieve a model describing the sorption mechanisms of dissolved matter of surface waters onto nanoparticles. Such studies can eventually lead us to a better understanding of the fate of the released nanoparticles under natural conditions.

Zusammenfassung

Der boomende Weltmarkt für Nanomaterialien hat in den letzten Jahrzehnten zu einer unvermeidlichen Emission dieser Materialien in die aquatische Umwelt geführt; daher ist das Verständnis ihrer physikalischen, chemischen und biologischen Umwandlungen für Umweltwissenschaftler zu einem wichtigen Anliegen geworden. Trotz großer Anstrengungen, die unternommen wurden, um die Mobilität, den Verbleib und die Risikobewertung von z. B. TiO_2-Nanopartikeln zu verstehen, ist es immer noch unklar, ob die unter kontrollierten Laborbedingungen erzielten Ergebnisse auf realistisch freigesetzte Nanopartikel in der aquatischen Umwelt verallgemeinert werden können, da die komplexe Dynamik der Umweltbedingungen unter kontrollierten Bedingungen nicht vollständig reproduzierbar ist.

In der vorliegenden Studie haben wir einen neuen Ansatz vorgeschlagen, um TiO_2-Nanopartikel den Umweltbedingungen natürlicher Oberflächengewässer auszusetzen, indem wir Dialysemembranen als passive Reaktoren verwenden. Die Funktion dieser Reaktoren beruht auf der Durchlässigkeit der Membran für die gelösten Stoffe des Oberflächenwassers, während die TiO_2-Nanopartikel die Membran nicht passieren. Diese Systeme haben den Vorteil, dass, obwohl die Komplexität und zeitliche Variabilität der meisten Umweltparameter von Oberflächengewässern innerhalb der Reaktoren reproduzierbar sind, kolloidale und partikuläre Interferenzen getrennt bleiben. Außerdem wird in den Dialysebeuteln nach der Einwirkung von Oberflächenwasser keine signifikante Verringerung der Porengröße, d. h. kein Membranfouling, beobachtet, was die Effizienz des Systems bestätigt.

Wir nutzten diese Reaktoren, um Nanopartikel in Oberflächengewässer einzubringen, und untersuchten, welchen Einfluss die physikalisch-chemischen Parameter der Oberflächengewässer auf die Bildung einer natürlichen Beschichtung auf Nanopartikeln haben. Dazu wurden Dialysebeutel verwendet, um TiO_2-Nanopartikel in situ zehn verschiedenen Oberflächengewässern im Frühjahr und Sommer 2019 auszusetzen. Aufgrund der Komplexität der natürlichen gelösten Stoffe in den Oberflächengewässern sowie ihrer geringen natürlichen Konzentrationen mussten wir eine Kombination aus analytischen Techniken und multivariater Datenanalyse verwenden, um die Beschichtungen zu untersuchen. Die anfänglichen Ergebnisse ähnelten den in der Literatur veröffentlichten laborkontrollierten Expositionsstudien, die zeigen, dass der pH-Wert, die elektrische Leitfähigkeit und die Ca^{2+}-Mg^{2+} Konzentration die drei wichtigsten Parameter von Oberflächengewässern sind, die die Bildung von Belägen steuern. Dennoch stießen wir auf ein Phänomen, das unter Laborbedingungen übersehen wurde: Natürliche Beläge setzen sich nicht nur aus organischen Stoffen (DOM: gelöste organische Stoffe), sondern auch aus anorganischen Stoffen (Karbonat) zusammen, was bedeutet, dass ihre realistischen Beläge komplexer sind als in den bisherigen Studien beschrieben.

Der zweite Teil dieser Arbeit konzentrierte sich auf die Untersuchung der Wechselwirkungen von realistischeren Nanopartikeln (extrahierte TiO_2-Nanopartikel aus 11 Sonnenschutzmitteln) mit DOM. Mithilfe von ToF-SIMS in Kombination mit einer hochdimensionalen Datenanalyse versuchten wir, ein allgemeines DOM-Sorptionsmuster unter den TiO_2-Nanopartikeln zu finden, da das Auffinden dieses Musters letztendlich einen Weg zur Bewertung des Verbleibs von (realistischeren) Nanopartikeln in der aquatischen Umwelt eröffnen könnte. Im Gegensatz zu unseren Erwartungen zeigten die Ergebnisse ein einzigartiges Sorptionsmuster für jedes Sonnenschutzmittel, das durch die ursprünglichen Spezifikationen der Sonnenschutzmittel gesteuert wird, was bedeutet, dass das Sorptionsmuster jedes Sonnenschutzmittels einzeln untersucht werden sollte. Im nächsten Schritt dieser Studie haben wir mit Hilfe von Random Forest die wichtigsten Fragmente von DOM extrahiert, die auf jedem Sonnenschutzmittel sorbiert wurden, und anschließend versucht, diese wichtigen Massen chemischen Fragmenten zuzuordnen. Um ein umfassendes Verständnis der Wechselwirkungen von freigesetztem n-TiO_2 in der aquatischen Umwelt zu erlangen, werden wir in zukünftigen Studien unsere Beschichtungsforschung auf verschiedene Arten von TiO_2-Nanopartikeln ausweiten, z. B. auf extrahierte Partikel aus Farben, wobei die Reaktionsmedien (Oberflächengewässer) eine breite Palette von Wasserparametern abdecken, die für verschiedene Ökosysteme repräsentativ sind. Unter Einsatz modernster Techniken wie der multivariaten Datenanalyse werden wir versuchen, ein Modell zu erstellen, das die Sorptionsmechanismen von gelösten Stoffen aus Oberflächengewässern an Nanopartikel beschreibt. Solche Studien können uns schließlich zu einem besseren Verständnis des Verbleibs der freigesetzten Nanopartikel unter natürlichen Bedingungen führen

1. Introduction

1.1. Engineered nanomaterials

Engineered nanomaterials (ENMs) as manufactured materials in small dimensions (1-100 nm range at least in one dimension) have recently shown impressive applications not only in academic fields but also in industry and consumer products.[1–7] ENMs are applied in a wide variety of products, e.g. electronics, nutrition, cosmetics, and medical drug designing,[6] where new applications are continuing to be developed.[8] In 2017, they had a market value amounting to nearly 49 billion U.S. dollars worldwide with an increasing value in the following years.[9]

There are seven main classes for ENMs: carbonaceous nanomaterials, semiconductors, metal oxides, nanopolymers, nanoclays, emulsions, and metals.[10] The most produced ENMs worldwide are TiO_2, ZnO, FeO_x, AlO_x, SiO_2, CeO_2, Ag, quantum dots, carbon nanotubes, and fullerenes.[11] Among them, titanium dioxide nanoparticles (n-TiO_2), as the focus of this thesis, represent the second most important part of ENMs production worldwide (550 - 5500 t per year)[5] and are widely used in cosmetics, paint, food, and energy production. The global n-TiO_2 market was valued at 17 billion U.S. dollars in 2020.[9]

1.2. Release of n-TiO₂ to the Environment

The continuously growing number of products containing n-TiO_2 leads to increasing their release to the surrounding environments; hence, it no longer comes as a surprise when scientists monitor these nanoparticles during their production, usage, and end-of-life in aquatic environments.[12–19] Most of the released nanoparticles have industrial sources like the release of n-TiO_2 from construction and demolition landfills,[16] or paints by natural weathering.[18] However, releasing is not simply limited to industrial sources; the last time that you used n-TiO_2-containing sunscreens[17] while swimming or washed your white clothes, you released these nanoparticles to aquatic environments (in textiles, pigment TiO_2 is incorporated in most synthetic fibers as delustrant).[14]

It is shown that sufficiently high concentrations of the nanoparticles, for instance for n-TiO_2 higher than 1 mg/L,[20] could cause an adverse effect on aquatic organisms,[21–26] such as negative effects of nanoparticles on growing algae as the primary producers in aquatic environments.[27] The significant risk is the potential transfer and magnification in food webs. Zhu et al.[28] found a significant amount of n-TiO_2 accumulated in daphnia upon chronic exposure (21 d). Moreover, they provided evidence of the transfer of n-TiO_2 from daphnia to zebrafish in a simplified freshwater food chain which may alter the growing status of these organisms at both individual and population levels, posing risks to aquatic ecosystems.[29]

In addition to toxicity studies on the released n-TiO$_2$, investigations of the fate of these nanoparticles have also increased over the last decades. Overall, these studies focus on the environmental processes that dominantly affect the fate of n-TiO$_2$ including bioaccumulation, transport processes (such as sedimentation), and transformation processes.[6]

Among the environmental processes, transformation processes are divided into chemical (such as degradation, dissolution, and adsorption), physical (such as aggregation), and biological transformations (such as redox reactions between bacteria and nanoparticles).[30] It is critical to know that the abovementioned phenomena are not independent of each other where, for example, the formation of natural coating onto nanoparticles (transformation) can change the colloidal stability (transport) of the nanoparticles. Lynch et al.[31] showed in biological media, nanoparticles acquire a coating of biomolecules (proteins, lipids, polysaccharides) which alters surface characteristics and thereby colloidal stability which is a key factor controlling the transport and ultimate fate of nanoparticles in aqueous environments. Colloidal stability is dependent on particle size, shape, and crystalline structure as well as the surface chemistry of the nanoparticles modified by the surrounding medium.[32–34] Well-dispersed particles will be widely transported and have higher chances to cause potential harm to organisms while aggregated particles precipitate out and sediment while their transport and bioavailability will be greatly restricted.[35] Sharma et. al., showed that aggregation is affected by pH, and ionic strength of aqueous suspensions as well as the properties of nanoparticles such as their sizes.[36] It is also shown that the interactions of nanoparticles with organic or inorganic components of the aquatic environment (e.g., colloids) affect the stability of the particles.[37,38] He et. al. investigated the effect of fulvic acids (FA) on the colloidal stability of n-TiO$_2$ and reported that by increasing FA concentration, the absolute value of zeta potential of nano-TiO$_2$ increases and particle size decreases at all pH which promotes the colloidal stability of nanoparticles.[39] Working with synthetic and natural waters, Zhang et al.,[40] declared that despite the presence of moderately high concentrations of natural organic matter, which tends to stabilize n-TiO$_2$, the addition of 20 mM PO$_4^{3-}$ destabilized the particles in lake water probably due to complexation of phosphate ions with nanoparticles.

1.3. Formation of natural coating onto nanoparticles

Interactions of nanoparticles with dissolved materials of natural waters, such as natural organic matter (NOM), greatly affect the surface properties (coating) which ultimately change the mobility, fate, transport, and bioavailability of the nanoparticles in aquatic environments.[34,41–44] Jayalath et al.[45] showed that the adsorption of humic acid, as a ubiquitous component of NOM in the environment on n-TiO$_2$, alters the aggregation and modifies the zeta potential; thus,

potentially changing the bioavailability of n-TiO$_2$ in the environment

NOM comprise a heterogeneous mixture of biological matter, such as carbohydrates, lipids, amino acids, and nucleic acids, combined with the products of biotic and abiotic chemical reactions between NOM molecules or between NOM and inorganic constituents of water.[46] NOM is present in almost all aquatic ecosystems at concentrations typically ranging from 0.1 to 10 mg L^{-1};[47] their chemical properties vary significantly from one water body to another. The main fraction of NOM present in surface waters contains humic substances, which are responsible for the color of natural waters.[46] Numerous experimental studies have been performed in the last years to evaluate the interactions of n-TiO$_2$ with NOM and the corresponding mechanisms.[20,48–50] Typical interactions are classified into several types including electrostatic interaction, ligand exchange, hydrophobic interaction, hydrogen bonding, π–π attraction, and cation bridging. In most cases, more than one interaction is involved and the relative contributions may vary depending on the inherent nature of NOM, ENPs, and the solutes.[51] For example, in natural waters, NOM coexist with ions which can alter the stabilization effect of pure NOM onto nanooparticles. Liu et al.[52] explored the interactions between NOM and n-TiO$_2$ in aqueous solutions containing monovalent and divalent cations; the results depicted that Ca^{2+} might destabilize the TiO$_2$ nanoparticles in the presence of NOM while the mediating effect of Na$^+$ cation is insignificant. The destabilization effect of the divalent ions on the stability of n-TiO$_2$ is presumably due ion bridge effect between nanomaterials coated by humic acids.[53]

Different kinds of nalytical techniques have been used to characterize the formed natural coatings onto nanoparticles, [51] e.g., attenuated total reflectance Fourier transformation infrared (ATR-FTIR) spectroscopy was used to investigate the functional groups of the sorbed molecules.[45] Chen et al.[54] used two-dimensional Fourier transformation infrared correlation spectroscopy assisted by the fluorescence excitation-emission matrix method to explore the interaction mechanism of humic acid with n-TiO$_2$; they showed that the C=O bonds and C−O bonds of humic acids play important roles in their interaction with nanoparticles. Time-of-flight secondary ion mass spectrometry (TOF-SIMS), X-ray photoelectron spectroscopy (XPS), and atomic force microscope (AFM) have been also used to investigate the interactions of n-TiO$_2$ nanotubes with proteins.[55–57] Recently, Lechtenfeld et al. introduced laser desorption ionization Fourier- transform ion cyclotron resonance mass spectrometry (LDI-FT-ICR-MS) for direct analysis of NOM sorbed onto gold nanoparticles as a promising method to study the molecular composition of coated nanoparticles.[58]

1.4. Can lab results be extrapolated to natural conditions?

There is a multitude of studies about the sorption of dissolved matter of surface waters, e.g.,

NOM onto TiO_2 nanoparticles via laboratory-scale batch systems.[59–63] For instance, sorption isotherms in which the relationship between concentrations of a dissolved compound in solution and on a surface of particles is investigated at a constant temperature. Using sorption isotherms, Li et al.[64] investigated the effect of humic acids (HAs) with different sources (peat, sediment, and straw) on the sorption affinity of phenanthrene to HAs-coated n-TiO_2. The results showed a significant sorption difference for different HAs suggesting different properties of HAs can cause different orientations and structures of adsorbed HAs, subsequently affecting the accessibility of hydrophobic domains that control the sorption of phenanthrene. Since the structure of HAs changes based on the properties of the surrounding environment, such as pH, temperature, and background electrolyte,[65] the environmental conditions affect the sorption [66] where different media of surface waters lead to different interactions. The question that arises here is to what extent the ever-changing natural conditions of water media can be reproduced in the laboratory.

As a rule of thumb, if a person wants to investigate the effect of 10 parameters and plans to have 5 levels for each parameter, he/she should design 5^{10} experiments for a systematical design; imagine the level of complexity observed in nature where there are too many parameters to control and to vary. To provide a higher degree of complexity compared to lab conditions, mesocosm systems were designed as a small portion of the natural environment or artificially reconstituted environmental systems that are brought under controlled conditions.[67–69] Dauda et al.[70] used a mesocosm approach to study the effect of n-TiO_2 on phytoplankton indicating that the influence of n-TiO_2 on the phytoplankton community is dependent on the concentration of nitrogen. However, the variation of the parameters, relevance, and complexity of water media under environmental conditions are still difficult to reproduce under any controlled system (including mesocosms).

Another challenging point is about the nanoparticles since the interactions of n-TiO_2 in aquatic systems depend not only on receiving water environment but also on nanoparticles and their initial coatings. The emission scenario of nanoparticles to the environment is divided into three groups;[4] release during the production of raw material, release during use, and release after disposal. Interestingly, there is an extensive body of studies on the release of uncoated nanoparticles, such as P25,[36,42,54,63,71] while their emission is not more than 2% of the production volume. A great deal of emissions is contributed to the use phase and after disposal with modified surface properties.[4] For instance, n-TiO_2 in sunscreens are coated with aluminum coatings to shield against the harmful effects of hydroxyl radicals generated upon exposure of TiO_2 to UV radiation [72] which can drastically change the fate and toxicity of these nanoparticles.[73] To overcome this drawback, more recent studies have been done on T-Lite[74] (titanium dioxide UV

filters widely used in sunscreens) or TiO_2 nanomaterials coated with aluminum oxide and polydimethylsiloxane as starting materials used by the cosmetic industries.[75] For instance, Slomberg et al. investigated TiO_2 UV filters, with hydrophobic and hydrophilic surfaces. Nonetheless, due to the limited information on nanoparticles' surface chemistry in final products where the presence of the initial coating can affect their expected sorption mechanisms,[76] modeling the fate of these nanoparticles in aquatic environments is still difficult.

1.5. Formation of natural coating onto n-TiO₂ nanoparticles under environmental conditions: What water parameters influence the formation of natural coating?

This study represents the first steps to investigate the interactions of n-TiO_2 with dissolved matter of surface waters under realistic conditions. We developed a new method to investigate nanoparticles´ aging in aquatic environments (realistic water media). This system leads to an in-situ formation of natural coatings on nanoparticles which can simultaneously reproduce the complexity and the temporal variability of a large number of environmental parameters (e.g., DOM structure and composition, temperature, inorganic ions, and pH) inside the dialysis bags. Under these conditions, we investigated the influential parameters of surface waters leading to the formation of natural coatings.

1.5.1. Dialysis bags

Exposure of n-TiO_2 (P25) to natural waters is introduced in this thesis by using dialysis membranes based on the passive sampling concept. Passive sampling is an environmental monitoring technique in which analyte molecules of the sampled medium flow to a collecting medium as a result of a difference in chemical potentials.[77–79] Chapter 3 validates dialysis bags as field-deployable reactors to provide a realistic exposure of nanoparticles to dissolved organic matter (DOM) of river waters. It is shown that n-TiO_2 with a diameter of 20-50 nm, remain inside the cellulose ester dialysis bags (100 kD) while DOM can diffuse inside (Figure 1). Furthermore, natural colloids could not enter the bag which simplifies the extraction of the nanoparticles after exposure.[66]

Making use of the concept of dialysis bags, n-TiO_2 were exposed to 18 different surface waters and the exposed particles were further explored. The strength of relationship between each two variables can be investigated by correlation coefficient. However, due to the high correlations observed between several parameters, investigating the relationships between input and output variables, on the basis of one-to-one correlations, is not solely informative here. Therefore, a multivariate statistical approach (random forest) was used to predict the formation of the coating.

Chapter 4[80] defines the used methods to investigate the influential parameters to form a natural coating on n-TiO$_2$ and discusses the presence of organic and inorganic groups on the surface of nanoparticles after exposure to surface waters.
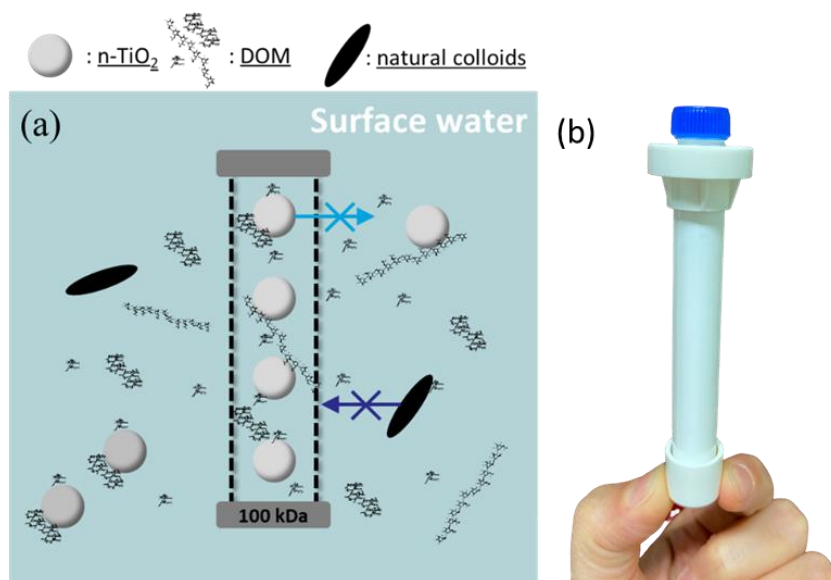

Figure 1: a) a cellulose ester dialysis bag. n-TiO$_2$ remain inside the membrane while DOM passed through the membrane. b) Repligen Float-A-Lyzer® Dialysis bags used in this study.

1.6. More realistic nanoparticles: exposure of n-TiO$_2$ extracted from sunscreens to DOM

To increase the environmental relevance of the nanoparticles, we investigated the sorption of DOM onto more realistic nanoparticles (in commercial sunscreens). Characterization of natural coatings in the mentioned systems is very challenging since, on the one hand, DOMs are supramolecular assemblies of several thousand different molecules[47] that require sensitive devices to detect sorption.[81] Galindo et al. detected about 5700 compounds for fulvic acids partitioned between the solution and alumina surface using ESI-FTMS (electrospray ionization-Fourier transform mass spectrometry).[82] On the other hand, the presence of initial coatings on the n-TiO$_2$ surface further complicates these systems. Therefore, there is still a lack of studies addressing the fate and effects of n-TiO$_2$ after processing into the final product.

Here, we investigated the sorption of DOM onto n-TiO$_2$ extracted from 11 different commercial sunscreens.[83] The extracted particles were exposed to a model DOM i.e., Suwannee River Fulvic Acid. Time of Flight Secondary Ion Mass Spectrometry (ToF-SIMS), as a surface-sensitive analysis, was used to analyze the surface of nanoparticles before and after exposure to fulvic acid. Due to the complexity of the reaction matrix, hundreds of ions were detected; however, considering them one by one would be time-consuming and could not uncover the patterns and trends in the acquired data. Hence, high-dimensional data analysis was applied to interpret the ToF-SIMS data. Random forest was used to extract the most important fragments for predicting

the presence of fulvic acids on the surface of the nanoparticles followed by an attempt to correlate the important masses to molecular structures. Chapter 5 depicts the sorption of fulvic acid onto titanium dioxide nanoparticles extracted from commercial sunscreens using ToF-SIMS and multivariate data analysis as the first steps towards a more complete characterization of natural coatings formed onto more realistic nanoparticles.

2. Objectives and Hypotheses

The main objective of this thesis is to investigate the interactions of n-TiO$_2$ with dissolved matter of surface waters under realistic conditions. Considering the complexity of these systems, we simplified the realistic conditions to either realistic water media i.e., river waters, or (more) realistic nanoparticles i.e., extracted n-TiO$_2$ from sunscreens (Figure 2).
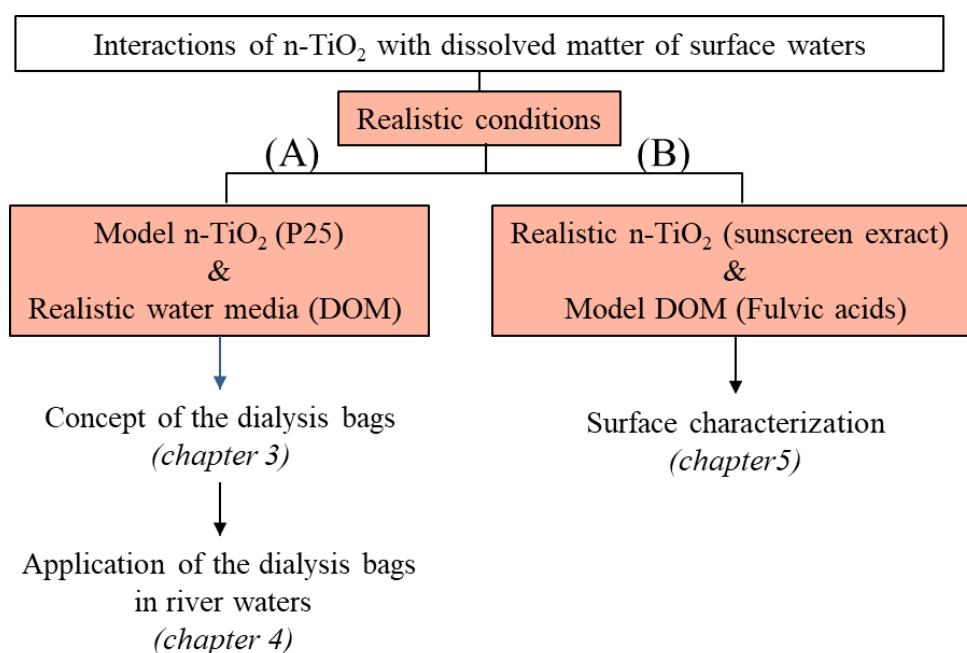
```
┌─────────────────────────────────────────────────────────────────┐
│     Interactions of n-TiO₂ with dissolved matter of surface waters │
└─────────────────────────────────────────────────────────────────┘
                    ┌─────────────────────┐
                    │  Realistic conditions │
                    └─────────────────────┘
        (A)                                      (B)
┌─────────────────────────┐      ┌─────────────────────────────┐
│   Model n-TiO₂ (P25)    │      │  Realistic n-TiO₂           │
│           &             │      │  (sunscreen exract)         │
│ Realistic water media   │      │           &                 │
│        (DOM)            │      │   Model DOM (Fulvic acids)  │
└─────────────────────────┘      └─────────────────────────────┘

  Concept of the dialysis bags        Surface characterization
        (chapter 3)                        (chapter5)

  Application of the dialysis bags
         in river waters
         (chapter 4)
```

Figure 2: The stepwise procedure in our study to investigate the interactions of n-TiO$_2$ with dissolved matter of surface waters under realistic conditions.

2.1. Part A: Realistic water media (river waters)

The objective of part A is to reveal the most relevant environmental factors of river waters directing the sorption of dissolved matter of surface waters onto n-TiO$_2$.

Hypothesis 1: Under natural conditions, despite the different physicochemical properties of surface waters, only a relatively small number of key parameters influence the formation of natural coatings onto n-TiO$_2$ nanoparticles.

Finding these parameters is in favor of saving the time and cost of the experiment, and simplifies the models used to describe the surface waters. To test this hypothesis, firstly, we developed a new method and showed dialysis bags' ability to provide realistic exposure conditions of nanoparticles to river waters (figure 3). To apply this method to environmental waters, the membrane needs to meet several requirements:

- The ability of the membrane to retain TiO$_2$ nanoparticles inside the bag while non-colloidal water components can diffuse through the bag.

- Robustness towards environmental variation (pH, temperature, water flow, and aquatic organisms)
- Constant permeability of the membrane during the exposure.

Chapter 3 presents the proof of concept of using dialysis bags and the validity of implementing this method to study the interactions of dissolved components of surface waters with engineered nanoparticles under environmental conditions.
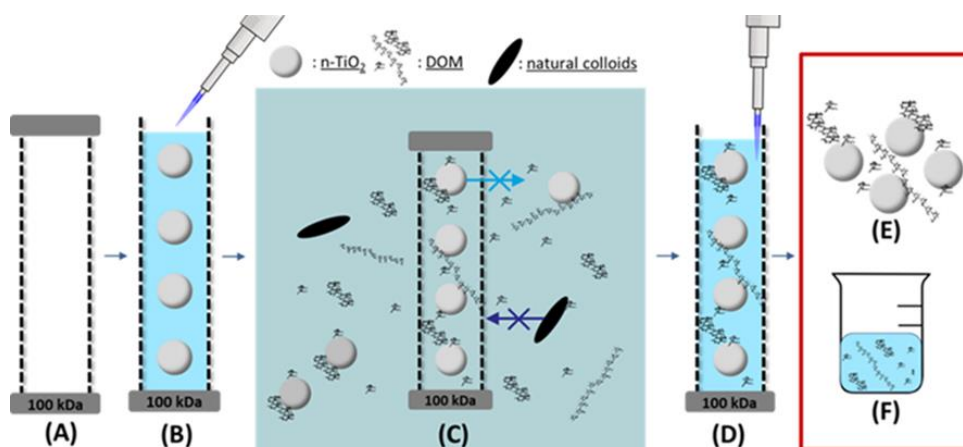

Figure 3: Schematic steps of using dialysis bags in surface waters to investigate the formation of natural coatings on P25. A) a dialysis bag (100 kDa), B) adding P25 suspension, C) placing the dialysis bag in river water; D) collecting the exposed nanoparticles, E) coated nanoparticles, F) DOM diffused inside the dialysis bag.

Based on the knowledge gained from Chapter 3, the dialysis bags were used to expose $n-TiO_2$, in situ, to different surface waters with contrasting physicochemical parameters. Hence, the physicochemical properties of 10 different water sites, located in Rheinland-Pfaltz, were measured in two different seasons (figure 4).

After exposing nanoparticles to surface waters, the formation of the natural coating was analyzed by ATR-IR, and the functional groups assigned by ATR-FTIR were confirmed by TGA, XPS, and 2D-IR (Figure A1). The observed functional groups were considered as a proxy for the formation of the natural coating. Subsequently, random forest as a multivariate statistical approach[84] was used to determine the importance of each input variable (water parameters) to form natural coatings. Chapter 4 presents the proof of the concept of hypothesis 1.
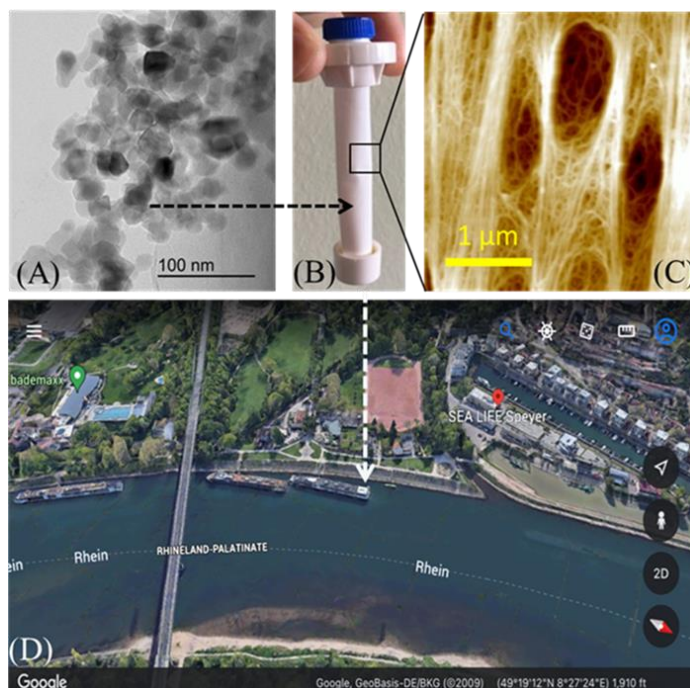
Figure 4: A) HR-TEM image of P25, B) Repligen dialysis bag C) AFM height image of the dialysis bag measured in fluid mode showing the pores of the membrane. D) Rhein River in Speyer as one of the selected locations to expose P25 to surface waters.

2.2. Part B: More realistic nanoparticles (extracted n-TiO$_2$ from sunscreens)

The objective of part B is to investigate the interactions of more realistic nanoparticles, extracted from 11 sunscreens (figure 5) with DOM to find a common sorption pattern among them.

Hypothesis 2: There is a general pattern of sorption of DOM on TiO$_2$ nanoparticles extracted from sunscreens regardless of the type of sunscreen. Hence, DOM-sorption patterns of TiO$_2$ nanoparticles in a random sunscreen can be generalized to all sunscreens.

Figure 5: 11 different sunscreens containing n-TiO$_2$. The nanoparticles were extracted and

consequently exposed to fulvic acids. The numbers on the bottles show the assigned names of the sunscreens. The complete list of sunscreens and their detailed specifications can be found in Chapter 5 (Sample 11 as the only sample containing ZnO was removed from the data analysis).

A mild extraction method with minimal surface modifications was used to extract n-TiO$_2$ from eleven commercial sunscreens.[83] The extracted nanoparticles were subsequently exposed to fulvic acids. Chapter 5 shows that a combination of ToF-SIMS and random forest can successfully differentiate between the surface of nanoparticles before and after exposure to fulvic acids while random forest can extract the most important fragments of fulvic acids sorbed onto each sunscreen. Based on our results, each sunscreen showed a unique sorption pattern leading to the rejection of hypothesis 2.

3. Validation of a field deployable reactor for in situ formation of NOM-engineered nanoparticle corona

Despite the numerous studies about the sorption of dissolved organic matter (DOM) onto nanoparticles, the extrapolation of laboratory results to environmental conditions is currently impossible. Indeed, the complex dynamics of DOM under variable environmental conditions are not completely reproducible under control conditions. In this study, we propose a different approach by exploring a method for exposing nanoparticles to realistic environmental conditions in natural river water by using dialysis membranes as passive reactors. Inside this reactor, the complexity and the temporal variability of a large number of environmental parameters (DOM structure and composition, temperature, inorganic ions, pH, etc.) are reproduced, while colloidal and particulate interferences remain separated. To verify this assumption, we determined the concentration of the water components and nanoparticles (n-TiO_2, 20–50 nm) inside and outside the reactor before and after exposure to river water. In river water, more than 90% of the n-TiO_2 nanoparticles remained inside the reactor while DOM retained its molecular composition/ characteristics after passing through the membrane (DOC, fluorescence EEM, and FT-ICR MS). For most elements and anions, the concentrations inside and outside the reactor did not differ, indicating a good permeability for inorganic constituents (IC, ICP-OES); however, the concentrations of Al, Fe, Mn, and nitrate were lower. Membrane fouling, in terms of pore size distribution, was investigated using NMR relaxometry and AFM in fluid mode; no significant reduction in pore size was observed under the applied conditions during seven days of exposure. Finally, ATR-FTIR and CHNS analysis of n-TiO_2 before and after exposure to the river water revealed that sorption of DOM occurred under field conditions. Therefore, we could demonstrate the validity and the potential of this method.

This article is part of the themed collection: Environmental Science: Nano Recent HOT Articles

About this collection

Here is a collection of recent *Environmental Science: Nano* articles which have been classified as 'HOT articles' due to receiving particularly high scores at peer review.

4. Influential parameters of surface waters on the formation of coating on TiO$_2$ nanoparticles under natural conditions

Formation of natural coatings on nanoparticles in aquatic media is highly influenced by the dynamic composition of the medium. Hundreds of research articles were dedicated to this question and an indepth understanding of the underlying mechanisms has been obtained for some materials. Nonetheless, it is still unknown to which extent these results obtained under controlled conditions in the laboratory can be extrapolated to environmental conditions. In this study, we used the recently introduced dialysis bag method to expose n-TiO$_2$ in situ to 18 surface waters with contrasting physicochemical parameters by varying the sampling location and season and characterized the resulting natural coatings. ATR-FTIR and 2D-IR spectroscopy (thermal perturbation), thermogravimetry, and X-ray photoelectron spectroscopy analyses of the exposed nanoparticles revealed clear differences in the composition of the natural coatings in the presence of both organic (carboxylate and aromatic groups) and inorganic (carbonate) components. Subsequently, multivariate data analysis (correlation matrix, principal component analysis, and random forest) was used to explore the relationships between surface water parameters and the composition of the natural coating; the results enabled us to identify pH, electrical conductivity, and Ca^{2+}–Mg^{2+} concentration as the three most important parameters for predicting the composition of the natural coating of TiO$_2$ nanoparticles.

This article is part of the themed collection: Environmental Science: Nano Recent HOT Articles

About this collection

Here is a collection of recent *Environmental Science: Nano* articles which have been classified as 'HOT articles' due to receiving particularly high scores at peer review.

5. Sorption of Fulvic Acids onto Titanium Dioxide Nanoparticles Extracted from Commercial Sunscreens: ToF-SIMS and High-Dimensional Data Analysis

Titanium dioxide nanoparticles (n-TiO_2) are common ingredients of sunscreens and are often released into surface waters during usage. Once released, the surface chemistry of n-TiO_2 changes by interacting with dissolved organic matter (DOM). In previous studies, these interactions were investigated using model n-TiO_2 and; therefore, do not account for the complex composition of the coating of n-TiO_2 aged in sunscreens. Taking advantage of a mild extraction method to provide more realistic nanoparticles, we investigated the potentials of time of flight-secondary ion mass spectrometry (ToF-SIMS) combined with high-dimensional data analysis to characterize the sorption of fulvic acids, as a model for DOM, on titanium dioxide nanoparticles extracted from ten different commercial sunscreens (n-$TiO_2 \subset$ sunscreen). Clustering analysis confirmed the ability of ToF-SIMS to detect the sorption of fulvic acids. Moreover, a unique sorption pattern was recognized for each n-$TiO_2 \subset$ sunscreen, which implied different fractionation of fulvic acids based on the initial specifications of nanoparticles, e.g., size, coating, etc. Furthermore, random forest was used to extract the most important fragments for predicting the presence of fulvic acids on the surface of n-$TiO_2 \subset$ sunscreen. Finally, we evaluate the potential of ToF-SIMS for characterizing the sorption layer.

This paper was chosen as Editors' Choice Paper (October 2022).

6. Synthesis, results, and outlook

In this work, we investigated the interactions of dissolved matter of surface waters with n-TiO$_2$; making an effort to bring the interaction conditions close to what occurs under realistic aquatic environments. Hence, we applied either dialysis bags (to provide realistic water media) or extracted n-TiO$_2$ from sunscreens (to provide more realistic nanoparticles). Figure 6 shows an overview of the findings of this thesis being elaborated in the following sub-chapters.
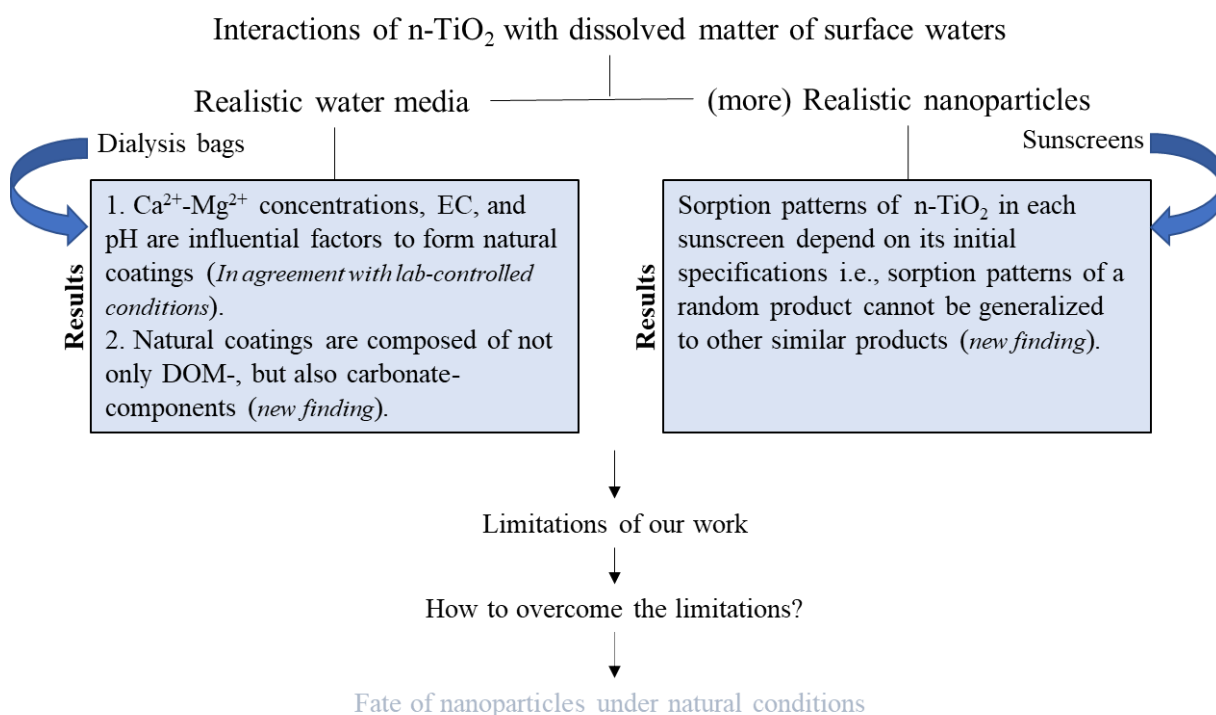
Interactions of n-TiO$_2$ with dissolved matter of surface waters

Realistic water media ———————— (more) Realistic nanoparticles

Dialysis bags
Sunscreens

Results
1. Ca^{2+}-Mg^{2+} concentrations, EC, and pH are influential factors to form natural coatings (*In agreement with lab-controlled conditions*).
2. Natural coatings are composed of not only DOM-, but also carbonate-components (*new finding*).

Results
Sorption patterns of n-TiO$_2$ in each sunscreen depend on its initial specifications i.e., sorption patterns of a random product cannot be generalized to other similar products (*new finding*).

Limitations of our work

How to overcome the limitations?

Fate of nanoparticles under natural conditions

Figure 6: Schematic overview of the findings of this study. Overcoming the limitations of this work can be a precious guide to understand the fate of nanoparticles under natural conditions.

6.1. Sorption studies using dialysis bags (realistic water media)

In the first part of our studies, we could successfully develop a new method that enabled us to expose n-TiO$_2$ (P25) to natural conditions of different river waters. Investigating the sorption interactions under the proposed conditions of such systems benefit from:

- Realistic conditions: Dialysis bags can provide realistic conditions for in-situ exposure of nanoparticles to surface waters, i.e., the exposed water media are surface waters with their natural characteristics.
- Cost and time effective: Performing sorption experiments in the lab which requires hundreds of experiments to cover all the water parameters under natural conditions, or designing (in-door) mesocosm is time and money-consuming. In comparison, the preparation, installation, and application of dialysis bags are cost and time effective.
- Worldwide application possibility: Considering the specification of dialysis bags, they

have the potential to be used in any water media around the world. In other words, the same sorption experiments in Germany can be conducted in other countries with different ecosystems, e.g., India. Conducting such experiments benefits from having a comprehensive water specification which leads to more realistic sorption models.

6.1.1 Were our results (realistic water media) in agreement with the literature?

Making use of this method, we could show that under natural conditions Ca^{2+}-Mg^{2+} concentrations, EC, and pH are three influential parameters controlling the formation of natural coating onto nanoparticles. The effects of these parameters have been already shown in the sorption experiments conducted under lab conditions.[61] For instance, pH is already introduced as an effective variable in occurring sorption where increasing the pH decreases the sorption of carboxylate on TiO_2 as a consequence of increasing the negative surface charge density of n-TiO_2.[85] At low pH, electrostatic attraction is a driving force to adsorb humic acid on n-TiO_2; while at high pH, ligand exchange yields inner-sphere complexes.[86] Previous studies have also shown the influence of bivalent cations and EC (correlated to dissolved salts of surface waters e.g., calcium, and magnesium) on sorption. For instance, it is observed that in the presence of Ca^{2+} and neutral pH, cation bridging affects the coating formation.[87]

It is important to mention that, in our study, random forest shows the importance of each parameter (input) to form the natural coating (output). However, it is not capable of showing how these parameters affect the coating. For example, although it introduces pH as an important factor, it does not clarify whether increasing or decreasing pH leads to the formation of a natural coating.

Interestingly, we came across a unique outcome which has been ignored in previous studies; the presence of calcium carbonate in natural coating revealing that natural coatings are not only composed of organic components, such as carboxylic groups but also inorganic carbons (chapter 4). Although there are studies about interactions of ENPs with both organic and inorganic ligands,[88] or the stability of TiO_2 nanoparticles, in the presence of Ca^{2+}-NOM bridges, has been already investigated under environmentally relevant conditions,[89] to the best of our knowledge, the simultaneous presence of these constitutes on natural coatings has not been mentioned elsewhere. This lack of information is probably due to the complicity of organic-inorganic systems and the subsequent difficulties to control the reaction conditions during the simultaneous use of carbonate and NOM. Firstly, the concentration distribution of various carbonate species in aqueous solution varies noticeably with solution pH where H_2CO_3 and HCO_3^- are the dominant species in acidic solutions, while CO_3^{2-} species predominates in basic solutions.[90] As the samples are in contact with the air, carbon dioxide gas can dissolve in water and change the

pH. Secondly, there are high correlation among the water variables where changing one specific parameter, influences other parameters. For instance, Coto et al.[91] showed that the solubility of calcium carbonate is highly dependent on temperature, pressure, and the presence of NaCl in the medium; moreover, the CO_2 partial pressure has a strong effect because there is a direct relation with solution pH that modify the number of ionic species present in the aqueous solution, and hence increasing the solubility of calcium carbonate. On the other hand, NOM structure can also vary based on different water parameters such as pH. For instance, the hydrophobicity of the NOM samples decreases with increasing content and strength of acidic groups.[92] Controlling all the parameters in the lab can be very difficult (or even impossible) which shows the efficiency of our method in conducting the experiments under natural conditions.

It is noteworthy that a detailed mechanistic description of the formation of the coating is beyond the aim of this thesis. Although we could detect that the presence of calcium carbonate on natural coatings is correlated to the saturation index (SI) of calcium carbonate in surface waters which can be a sign of precipitation.[80] In agreement with this result, Zhu et al. showed that in freshwaters, a negatively charged surface can adsorb available metal ions, such as Ca^{2+}, which increases the concentration of surrounding Ca^{2+}; consequently, when carbonate is available, oversaturation occurs.[93] Nonetheless, sorption interactions must not be underestimated in such systems. In aqueous conditions, $CaCO_3$ and TiO_2 particles can interact through their surface hydroxyls,[94] where calcium complexations can enhance the NOM-sorption interactions.[95] One suggestion here for future studies can be using XRD analysis; in case $CaCO_3$ presents in crystalline form, XRD can detect if carbonate is simply precipitated onto n-TiO_2 or if they react with each other.[96]

6.2. Sorption studies on n-TiO₂ extracted from sunscreens (more realistic nanoparticles)

We dedicated the second phase of our studies to the interactions of more realistic n-TiO_2 extracted from different sunscreens with Suwannee River Fulvic Acid (SRFA). For the sake of simplicity, we will refer to "sunscreen" for denoting n-TiO_2 extracted from sunscreen.

It is estimated that sunscreens make up about 25% of the nano-TiO_2 market share;[6] hence, many studies have been recently conducted to investigate the fate of sunscreen-derived titanium dioxide nanoparticles in aquatic environments.[97] The common point of these studies is using either model n-TiO_2[74] or one type (brand) of sunscreen.[98] However, it is not yet clear if the sorption/fate studies of one type of sunscreen can be generalized to other sunscreens. A negative answer to this question can make a big challenge for environmental scientists since it implies that the sorption/fate of each product should be investigated individually.

In Chapter 5, taking advantage of ToF-SIMS, as a surface-analysis technique,[99] and high-

dimensional data analysis performed on increased-mass intensities, we could show that each sunscreen depicts a unique sorption pattern after exposure to fulvic acids. Interestingly, cluster analyses showed that, for each sunscreen, exposed nanoparticles tend to cluster close to the initial sunscreens which shows the dominance of the composition of each sunscreen in the sorption process.

It is worth mentioning that the sunscreen experiments were performed under lab conditions and the results cannot be yet generalized to natural conditions. Moreover, based on our experiments, we cannot declare which specifications (e.g., ingredients of the sunscreen, size, shape, and charge of nanoparticles) are the sorption controlling factors. Considering the variation of commercial sunscreens in the market, investigation of a specific parameter, e.g., the effect of the size of nanoparticles on the sorption, seems to be impossible. Such studies require lab-prepared sunscreens; for instance, preparing sunscreens with the same ingredients but different sizes of n-TiO_2.

6.3. Limitations of this thesis

Due to the complexity of the reaction media and the novelty of the study, we used different analytical techniques to show the proof of concept. For instance, membrane fouling of the dialysis bags was investigated using two different methods namely ^{1}H-NMR relaxometry and AFM (chapter 3), or the formation of natural coatings onto nanoparticles was explored by ATR-FTIR, 2D-IR, XPS, and TGA (chapter 4). Furthermore, multivariate data analysis was used to interpret the acquired complex data sets (chapter 5) and/or to find important variables influencing the reactions (chapter 4). However, we face some limitations in the present work:

- Limited observations in field experiments: In Chapter 4, 10 different surface waters (in two seasons) were chosen as exposure sites; however, they were covering rather a narrow range of water parameters. A comprehensive study needs more observations to cover a wide range of possible environmental parameters.

- Characterization of DOM of surface waters: In Chapter 3, we investigated the major compound-class distribution of Queich river by FT-ICR-MS. However, a thorough characterization of the chemical structure of DOM of all surface waters is still missing. Achieving this point can be helpful to reveal the chemical formula of the available DOM in each surface water and predict the interactions of DOM with nanoparticles.

- Nanoparticles: Our investigations were performed either on P25 as a model of TiO_2 nanoparticle (chapters 3 and 4), or the more realistic n-TiO_2 in sunscreens (chapter 5). However, to be able to have a model of TiO_2 nanoparticles, studies should be done on different types of these nanoparticles such as NM-103 or the aged nanoparticles in paints.

- Surface characterization: Characterization of the surface of the nanoparticles before and after exposure to river waters is a vital step to identify the natural coatings. However, it is still elusive due to the complexity and heterogeneity of natural water compositions, and the inadequate characterization methods. Some problems are the low concentrations of the compound in the coating that can be less than the limit of the detection of the analytical instruments or probable inhomogeneity of the coatings (e.g., the simultaneous presence of organic and inorganic compounds).[80] On the other hand, based on the volumetric size of the dialysis bags, limited amounts of nanoparticles can be exposed to river waters (few milligrams) where some analytical instruments require a few hundred milligrams of samples for each measurement (e.g., solid-state-NMR needs at least 100 mg).

6.4. How to overcome the limitations?

In the last parts, we could show the potential of this thesis to investigate the formation of natural coating onto TiO_2 nanoparticles; however, there is still a challenging path to have thorough knowledge about coating characteristics and the sorption mechanisms. The following suggestions can overcome the drawbacks of this work (Figure 7):
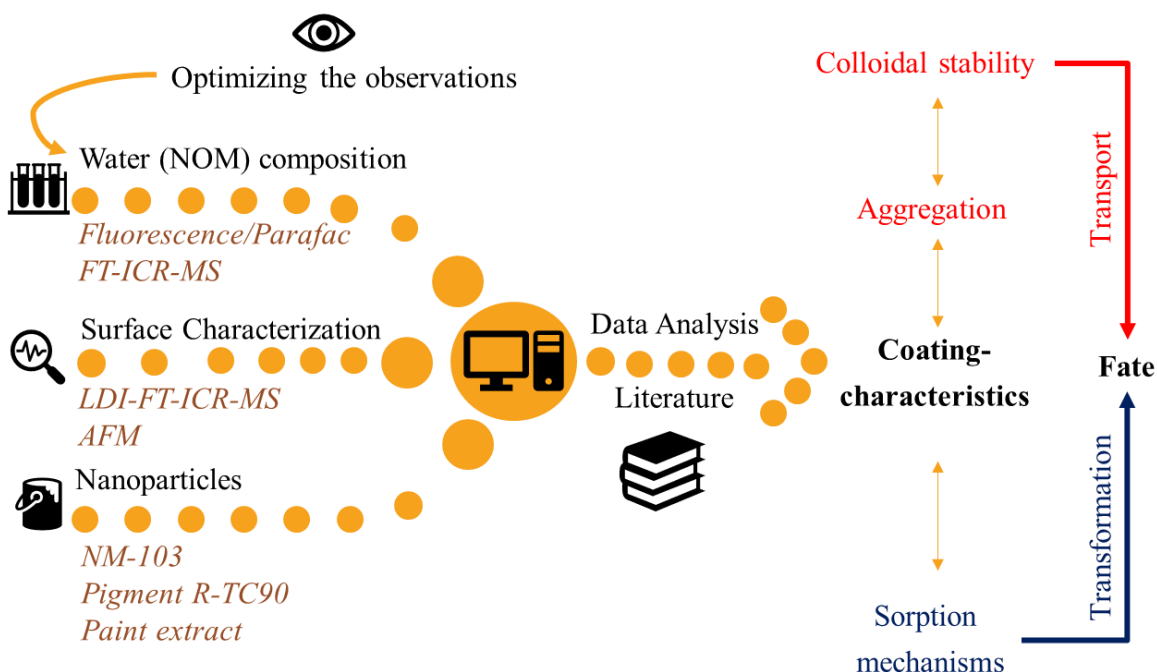

Figure 7: The scheme of future studies to overcome the shortcomings of this thesis which can subsequently lead us to understanding the fate of TiO_2 nanoparticles under natural conditions.

- Optimizing the observations: The first challenge is selecting surface waters to perform the sorption experiments. On the one hand, the number of observations should be comparable to the number of variables (measured water parameters); on the other hand,

the selected sites should be representative of different water media with contrasting parameters which can cover a wide range of water parameters. Furthermore, the number of observations should be practically logical since the field experiments of different sites should be done in close time intervals. Data analysis can be a key point to deal with this challenge. Hence, initially, the physicochemical properties of several (e.g., 100 sites) sites are measured. Subsequently, making use of data analysis e.g. clustering, the number of sites is reduced in a way that the final selected (e.g., 20 sites) sites ideally reflect the environmental conditions of all the initial sites.

- Water (NOM) composition: Other than the techniques used in our previous studies, FT-ICR-MS can be used to provide an in-depth molecular analysis of the water samples and access the molecular weight fraction of heteroatoms, and aromaticities of the water media exposed to the nanoparticles. Moreover, as a complementary study, the fluorescence EEM-Parafac method will be used to explore the possibility of the assignments of the obtained molecular fractions (obtained from FT-ICR-MS) to organic fluorophore groups, i.e., proteins, humic acids, fulvic acids.

- Nanoparticles: To provide a plausible range of environmentally relevant exposure, different types of n-TiO$_2$ including model and more realistic particles (P25, NM-103, Pigment R-TC90, sunscreen and paint extracts) are investigated in each selected site.

- Coating characterization: After exposure of nanoparticles to surface waters, they are characterized by the techniques described in Chapter 4. Moreover, the state-of-the-art technique of LDI-FT-ICR-MS,[58] which can directly analyze molecules attached to nanoparticle surfaces, is used to analyze the surface of exposed nanoparticles. In addition, atomic force microscopy (AFM)[100] is going to be used to evaluate the nanoparticles (single particles) before and after exposure to surface waters to compare their adhesion analyzed by the force-distance curves.[101]

Combining these methods with multivariate data analysis, we are going to provide a more realistic understanding of the formation of natural coatings on nanoparticles. The acquired knowledge about the surface properties of nanoparticles and the properties of the water media is used in subsequent aggregation studies to reveal the stability and deposition behavior of these nanoparticles. The results of this study as long as performing the aggregation experiments under natural conditions and combining the results with the literature can be a path to a comprehensive understanding of sorption mechanisms (transformation), and colloidal stability (transport) of n-TiO$_2$ under natural conditions leading to a better understanding of the fate of nanoparticles in aquatic environments.

6.5. Other Potentials of this Work

Using dialysis bags benefits from performing the experiments under natural conditions; hence, they have the potential of being used in different fields of study. Firstly, although we investigated n-TiO$_2$ nanoparticles; other (nano) particles, insoluble in water such as silica nanoparticles,[102] can be the subject of investigation as long as the particles remain inside and the target solutes, such as DOM, are capable of diffusing through the bag. Secondly, we used dialysis bags to explore the surface waters; however, other reaction media e.g., ground waters as drinking water supplies[103] or wastewater treatment plants, as the important point sources for the discharge of nanoparticles to natural surface waters,[20] could be also investigated. Dialysis bags can be even used in wet soils, as the reaction media, where soil organic matter (SOM) could diffuse inside the bag through the membrane. Thirdly, In this work, we used cellulose esters (100 kD) as the membrane; other sizes or other types of dialysis membranes, e.g. polysulfones,[104] could also be evaluated.

Using dialysis bags can be extrapolated to polymer studies including releasing of microplastics into surface waters as the new concern of our century. Microplastics transport through rivers into the sea; however, the environmental fate of riverine microplastics is still unclear.[105] Wang et al.[106] investigated the interactions of microplastics with antibiotics (as two major types of pollutants) in aquatic environments; they could show that environmental factors (such as pH, ionic strength, and dissolved organic matter) affect the sorption of antibiotics onto microplastics. Using dialysis bags, such interactions can be investigated under natural conditions.

Dialysis bags can be also a tool for toxicological studies where microorganisms, such as daphnia, are trapped inside the bags and getting exposed to natural environments. Cupi et al.[107] showed the influence of pH and media composition on the immobilization of Daphnia Magna. Conducting similar experiments under natural conditions can lead to more realistic results.

It is worth mentioning that any new application of dialysis bags (e.g., changing the size, type, used particles, and exposing media) requires a comprehensive study to validate the efficiency of the membrane under the applied conditions. Chapter 3 can be used as a guideline to examine the validation of dialysis bags for different applications.

7. References

1   R. A. Yokel and R. C. MacPhail, *Journal of Occupational Medicine and Toxicology*, 2011, **6**, 1–27.

2   M. Baalousha, G. Cornelis, T. Kuhlbusch, I. Lynch, C. Nickel, W. Peijnenburg and N. Van Den Brink, *Environmental Science: Nano*, 2016, **3**, 323–345.

3   C. Crézé, M. François, N. B. Hopf, V. Dorribo, J.-J. Sauvain, E. Bergamaschi, G. Garzaro, M. Domat, J. Friesl, E. Penssler and others, *International journal of environmental research and public health*, 2021, **18**, 3851.

4   A. A. Keller, S. McFerran, A. Lazareva and S. Suh, *Journal of nanoparticle research*, 2013, **15**, 1–17.

5   V. Adam, S. Loyaux-Lawniczak and G. Quaranta, *Environmental Science and Pollution Research*, 2015, **22**, 11175–11192.

6   S. Heilgeist, R. Sekine, O. Sahin and R. A. Stewart, *Water*, 2021, **13**, 734.

7   F. Gottschalk, C. Lassen, J. Kjoelholt, F. Christensen and B. Nowack, *International journal of environmental research and public health*, 2015, **12**, 5581–5602.

8   E. R. Bandala and M. Berli, *Materials Science for Energy Technologies*, 2019, **2**, 29–40.

9   Titanium dioxide market will reach 17 billion U.S. dollars by 2020, http://www.sino-tio2.com/home.php?m=&c=news&a=show&id=64, (accessed 9, 2022).

10 G. E. Batley, J. K. Kirby and M. J. McLaughlin, *Accounts of chemical research*, 2013, **46**, 854–862.

11 F. Piccinno, F. Gottschalk, S. Seeger and B. Nowack, *Journal of nanoparticle research*, 2012, **14**, 1–11.

12 A. Praetorius, M. Scheringer and K. Hungerbühler, *Environmental science & technology*, 2012, **46**, 6705–6713.

13 M. A. Maurer-Jones, I. L. Gunsolus, C. J. Murphy and C. L. Haynes, *Analytical chemistry*, 2013, **85**, 3036–3049.

14 L. Windler, C. Lorenz, N. von Goetz, K. Hungerbuhler, M. Amberg, M. Heuberger and B. Nowack, *Environmental science & technology*, 2012, **46**, 8181–8188.

15 M. Bundschuh, J. Filser, S. Lüderwald, M. S. McKee, G. Metreveli, G. E. Schaumann, R. Schulz and S. Wagner, *Environmental Sciences Europe*, 2018, **30**, 6.

16 R. Kaegi, A. Englert, A. Gondikas, B. Sinnet, F. von der Kammer and M. Burkhardt, *NanoImpact*, 2017, **8**, 73–79.

17 F. Gottschalk and B. Nowack, *Journal of Environmental Monitoring*, 2011, **13**, 1145–1155.

18 L. Reijnders, *Polymer degradation and stability*, 2009, **94**, 873–876.

19 J. Liu, K. G. Pennell and R. H. Hurt, *Environmental science & technology*, 2011, **45**, 7345–7353.

20 X. Shi, Z. Li, W. Chen, L. Qiang, J. Xia, M. Chen, L. Zhu and P. J. Alvarez, *NanoImpact*, 2016, **3**, 96–103.

21 V. Lazic, M. Radoicic, Z. Saponjic, T. Radetic, V. Vodnik, S. Nikolic, S. Dimitrijevic and M. Radetic, *Cellulose*, 2015, **22**, 1365–1378.

22 Z. Wang, L. Zhang, J. Zhao and B. Xing, *Environmental Science: Nano*, 2016, **3**, 240–255.

23 A. Gondikas, F. von der Kammer, R. Kaegi, O. Borovinskaya, E. Neubauer, J. Navratilova, A. Praetorius, G. Cornelis and T. Hofmann, *Environmental Science: Nano*, 2018, **5**, 313–326.

24 Z. Bo, S. Y. Avsar, M. K. Corliss, M. Chung and N.-J. Cho, *Journal of hazardous materials*, 2017, **339**, 264–273.

25 Y. Zhao, K. Lin, W. Zhang and L. Liu, *Journal of Environmental Sciences*, 2010, **22**, 1987–1992.

26 D. Sánchez-Quiles and A. Tovar-Sánchez, *Environment international*, 2015, **83**, 158–170.

27 H. M. Abdel-Latif, M. A. Dawood, S. Menanteau-Ledouble and M. El-Matbouli, *Ecotoxicology and Environmental Safety*, 2020, **200**, 110776.

28 X. Zhu, Y. Chang and Y. Chen, *Chemosphere*, 2010, **78**, 209–215.

29 X. Zhu, J. Wang, X. Zhang, Y. Chang and Y. Chen, *Chemosphere*, 2010, **79**, 928–933.

30 G. V. Lowry, K. B. Gregory, S. C. Apte and J. R. Lead.

31 I. Lynch, A. Ahluwalia, D. Boraschi, H. J. Byrne, B. Fadeel, P. Gehr, A. C. Gutleb, M. Kendall and M. G. Papadopoulos, *BioNanoMaterials*, 2013, **14**, 195–216.

32 M. Kosmulski, *Advances in colloid and interface science*, 2002, **99**, 255–264.

33 K. A. Dunphy Guzman, M. P. Finnegan and J. F. Banfield, *Environmental science & technology*, 2006, **40**, 7688–7693.

34 F. Loosli, P. Le Coustumer and S. Stoll, *Science of the Total Environment*, 2015, **535**, 28–34.

35 D. Lin, X. Tian, F. Wu and B. Xing, *Journal of environmental quality*, 2010, **39**, 1896–1908.

36 V. K. Sharma, *Journal of Environmental Science and Health Part A*, 2009, **44**, 1485–1495.

37 T. L. Moore, L. Rodriguez-Lorenzo, V. Hirsch, S. Balog, D. Urban, C. Jud, B. Rothen-Rutishauser, M. Lattuada and A. Petri-Fink, *Chemical Society Reviews*, 2015, **44**, 6287–6305.

38 W. Wu, M. Queiroz and N. Mohallem, *Journal of Coatings Technology and Research*, 2016, **13**, 277–286.

39 H. He, B. Wu and C. Yang, *International Journal of Environmental Science and Technology*, 2019, **16**, 7275–7284.

40 C. Zhang, J. Lohwacharin and S. Takizawa, *Scientific Reports*, 2017, **7**, 9943.

41 K. Yang, D. Lin and B. Xing, *Langmuir*, 2009, **25**, 3571–6.

42 P. Wang, *International Journal of Environmental Sciences & Natural Resources*, 2017, **1**, 157–162.

43 F. Loosli, L. Vitorazi, J.-F. Berret and S. Stoll, *water research*, 2015, **80**, 139–148.

44 M. Drosos, M. Ren and F. H. Frimmel, *Applied Catalysis B: Environmental*, 2015, **165**, 328–334.

45 S. Jayalath, H. Wu, S. C. Larsen and V. H. Grassian, *Langmuir*, 2018, **34**, 3136–3145.

46 G. Zhu, Y. Bian, A. S. Hursthouse, P. Wan, K. Szymanska, J. Ma, X. Wang and Z. Zhao, *Journal of fluorescence*, 2017, **27**, 2069–2094.

47 A. Philippe and G. E. Schaumann, *Environmental science & technology*, 2014, **48**, 8946–8962.

48 G. E. Schaumann, A. Philippe, M. Bundschuh, G. Metreveli, S. Klitzke, D. Rakcheev, A. Grün, S. K. Kumahor, M. Kühn, T. Baumann and others, *Science of the Total Environment*, 2015, **535**, 3–19.

49 C. Larue, H. Castillo-Michel, S. Sobanska, N. Trcera, S. Sorieul, L. Cécillon, L. Ouerdane, S. Legros and G. Sarret, *Journal of hazardous materials*, 2014, **273**, 17–26.

50 P. Cervantes-Avilés, J. Ida, T. Toda and G. Cuevas-Rodriguez, *Journal of environmental management*, 2018, **222**, 227–233.

51 S. Yu, J. Liu, Y. Yin and M. Shen, *Journal of Environmental Sciences*, 2018, **63**, 198–217.

52 H. Liu, J. Lu, T. Zheng, D. Liu and F. Cui, *Environmental Engineering Science*, 2018, **35**, 846–855.

53 W. Liu, W. Sun, A. G. Borthwick and J. Ni, *Colloids and Surfaces A: Physicochemical and Engineering Aspects*, 2013, **434**, 319–328.

54 W. Chen, C. Qian, X.-Y. Liu and H.-Q. Yu, *Environmental science & technology*, 2014, **48**, 11119–11126.

55 R. Lu, C. Wang, X. Wang, Y. Wang, N. Wang, J. Chou, T. Li, Z. Zhang, Y. Ling and S. Chen, *International journal of nanomedicine*, 2018, **13**, 2037.

56 Y. Dong, X. Ji, A. Laaksonen, W. Cao, H. He and X. Lu, *Langmuir*, 2020, **36**, 9323–9332.

57 W. Phoohinkong, T. Foophow and U. Kitthawee, *Thai Journal of Nanoscience and Nanotechnology*, 2018, **3**, 1–9.

58 K. Giannopoulos, P. Benettoni, T. R. Holbrook, T. Reemtsma, S. Wagner and O. J. Lechtenfeld, *Environmental Science: Nano*, 2021, **8**, 2336–2346.

59 K. Yang and B. Xing, *Environmental science & technology*, 2009, **43**, 1845–1851.

60 X. Tan, X. Wang, C. Chen and A. Sun, *Applied Radiation and Isotopes*, 2007, **65**, 375–381.

61 P. Mwaanga, E. R. Carraway and M. A. Schlautman, *Environmental monitoring and assessment*, 2014, **186**, 8833–8844.

62 X. Wang, E. Ma, X. Shen, X. Guo, M. Zhang, H. Zhang, Y. Liu, F. Cai, S. Tao and B. Xing, *Environmental pollution*, 2014, **194**, 31–37.

63 S. L. Gora and S. A. Andrews, *Chemosphere*, 2017, **174**, 363–370.

64 Y. Li, C. Yang, X. Guo, Z. Dang, X. Li and Q. Zhang, *Chemosphere*, 2015, **119**, 171–176.

65 M. Avena, A. Vermeer and L. Koopal, *Colloids and Surfaces A: Physicochemical and Engineering Aspects*, 1999, **151**, 213–224.

66 N. Tayyebi Sabet Khomami, A. Philippe, O. J. Lechtenfeld, J.-M. Guigner, S. Heissler, G. E. Schaumann and others, *Environmental Science: Nano*, 2020, **7**, 486–500.

67 B. E. Vencalek, S. N. Laughton, E. Spielman-Sun, S. M. Rodrigues, J. M. Unrine, G. V. Lowry and K. B. Gregory, *Environmental Science & Technology Letters*, 2016, **3**, 375–380.

68 G. Metreveli, S. Kurtz, R. R. Rosenfeldt, F. Seitz, S. K. Kumahor, A. Grün, S. Klitzke, H.-J. Vogel, M. Bundschuh, T. Baumann and others, *Environmental Science: Nano*, 2021, **8**, 1771–1785.

69 M. Auffan, M. Tella, C. Santaella, L. Brousset, C. Paillès, M. Barakat, B. Espinasse, E. Artells, J. Issartel, A. Masion and others, *Scientific reports*, 2014, **4**, 1–7.

70 S. Dauda, A. M. Gabriel, O. F. Idris and M. A. Chia, *Journal of Applied Phycology*, 2020, **32**, 3123–3132.

71 C. Deiana, E. Fois, S. Coluccia and G. Martra, *The Journal of Physical Chemistry C*, 2010, **114**, 21531–21538.

72 J. Virkutyte, S. R. Al-Abed and D. D. Dionysiou, *Chemical Engineering Journal*, 2012, **191**, 95–103.

73 D. L. Slomberg, R. Catalano, F. Ziarelli, S. Viel, V. Bartolomei, J. Labille and A. Masion, *RSC Advances*, 2020, **10**, 8266–8274.

74 J. Labille, J. Feng, C. Botta, D. Borschneck, M. Sammut, M. Cabie, M. Auffan, J. Rose and J.-Y. Bottero, *Environmental Pollution*, 2010, **158**, 3482–3489.

75 C. Nickel, B. Hellack, A. Nogowski, F. Babick, M. Stintz, H. Maes, A. Schäffer and T. Kuhlbusch, *Environmental Research of the Federal Ministry for the Environment*.

76 X.-H. Guan, G.-H. Chen and C. Shang, *Journal of colloid and interface science*, 2006, **301**, 419–427.

77 T. Górecki and J. Namieśnik, *TrAC Trends in Analytical Chemistry*, 2002, **21**, 276–291.

78 A. Kot, B. Zabiegala and J. Namiesnik, *TrAC Trends in Analytical Chemistry*, 2000, **19**, 446–459.

79 J. Namieśnik, B. Zabiegała, A. Kot-Wasik, M. Partyka and A. Wasik, *Anal Bioanal Chem*, 2005, **381**, 279–301.

80 N. Tayyebi Sabet Khomami, P. M. Patel, C. P. Jusi, V. Trouillet, J. David, G. E. Schaumann and A. Philippe, *Environmental Science: Nano*, 2021, **8**, 3153–3166.

81 N. Tayyebi Sabet Khomami, A. Welle, S. Kunz and A. Philippe, *Coatings*, 2022, **12**, 335.

82 C. Galindo and M. Del Nero, *Environmental science & technology*, 2014, **48**, 7401–7408.

83 A. Philippe, J. Kosik, A. Welle, J.-M. Guigner, O. Clemens and G. E. Schaumann, *Environmental Science: Nano*, 2018, **5**, 191–202.

84 T. Hastie, R. Tibshirani, J. H. Friedman and J. H. Friedman, *The elements of statistical learning: data mining, inference, and prediction*, Springer, 2009, vol. 2.

85 F. Roncaroli and M. A. Blesa, *Physical Chemistry Chemical Physics*, 2010, **12**, 9938–9944.

86 M. Erhayem and M. Sohn, *Science of the Total Environment*, 2014, **470**, 92–98.

87 E. M. Murphy, J. M. Zachara, S. C. Smith, J. L. Phillips and T. W. Wietsma, *Environmental science & technology*, 1994, **28**, 1291–1299.

88 A. D. Dwivedi, S. P. Dubey, M. Sillanpää, Y.-N. Kwon, C. Lee and R. S. Varma, *Coordination Chemistry Reviews*, 2015, **287**, 64–78.

89 M. B. Romanello and M. M. F. de Cortalezzi, *Water research*, 2013, **47**, 3887–3898.

90 Y. Ku, W.-H. Lee and W.-Y. Wang, *Journal of Molecular Catalysis A: Chemical*, 2004, **212**, 191–196.

91 B. Coto, C. Martos, J. L. Peña, R. Rodriguez and G. Pastor, *Fluid Phase Equilibria*, 2012, **324**, 1–7.

92 P. K. Egeberg and J. J. Alberts, *Water research*, 2002, **36**, 4997–5004.

93 T. Zhu and M. Dittrich, *Frontiers in bioengineering and biotechnology*, 2016, **4**, 4.

94 H. Lin, Y. Dong and L. Jiang, *International Journal of Minerals, Metallurgy and Materials*, 2009, **16**, 592–597.

95 B. J. R. Thio, D. Zhou and A. A. Keller, *Journal of hazardous materials*, 2011, **189**, 556–563.

96 H. Tao, Y. He and X. Zhao, *Powder technology*, 2015, **283**, 308–314.

97 D. L. Slomberg, R. Catalano, V. Bartolomei and J. Labille, *Environmental Pollution*, 2021, **271**, 116263.

98 S. Heilgeist, R. Sekine, D. Clases, O. Sahin and R. A. Stewart, *ACS ES&T Water*.

99 D. R. Baer, D. J. Gaspar, P. Nachimuthu, S. D. Techane and D. G. Castner, *Analytical and bioanalytical chemistry*, 2010, **396**, 983–1002.

100 S. Gazze, I. Hallin, G. Quinn, E. Dudley, G. Matthews, P. Rees, G. Van Keulen, S. Doerr and L. Francis, *Nanoscale*, 2018, **10**, 520–525.

101 T. Eastman and D.-M. Zhu, *Langmuir*, 1996, **12**, 2859–2862.

102 W. Tan, K. Wang, X. He, X. J. Zhao, T. Drake, L. Wang and R. P. Bagwe, *Med Res Rev*, 2004, **24**, 621–38.

103 P. Wanner, *Chemosphere*, 2021, **264**, 128453.

104 M. Hayama, K. Yamamoto, F. Kohori and K. Sakai, *Journal of membrane science*, 2004, **234**, 41–49.

105 X. Xiong, C. Wu, J. J. Elser, Z. Mei and Y. Hao, *Science of the Total Environment*, 2019, **659**, 66–73.

106 Y. Wang, Y. Yang, X. Liu, J. Zhao, R. Liu and B. Xing, *Environmental Science & Technology*, 2021, **55**, 15579–15595.

107 D. Cupi, N. B. Hartmann and A. Baun, *Ecotoxicology and Environmental Safety*, 2016, **127**, 144–152.

8. Annexes
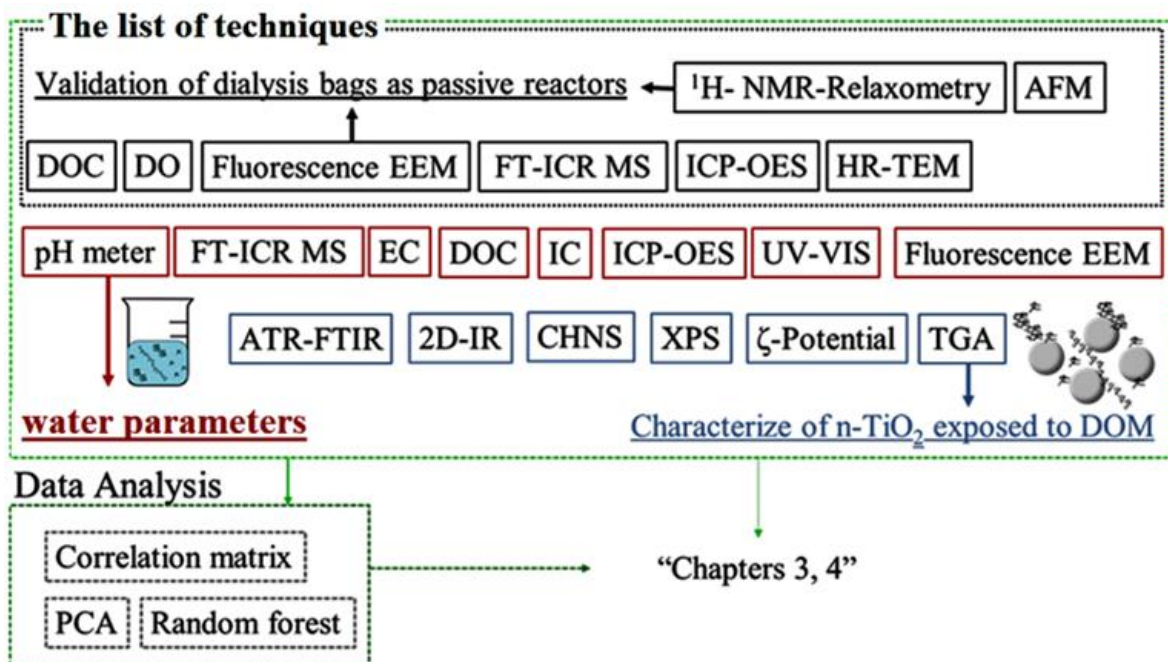
Figure A1. The used techniques and data analyses in chapters 3 and 4 (The complete names of the techniques with the corresponding information can be found in the appendix tables).

8.1. Tables of Abbreviations

Table 1: Abbreviations used in the text

abbreviation	
NOM	Natural organic matter
DOM	Dissolved organic matter
n-TiO$_2$	Titanium dioxide nanoparticles
SRFA	Suwannee River Fulvic Acid

Table 2: Analytics to validate dialysis bags

Abbreviations	Complete name	More information
ICP-OES	inductively coupled plasma-optical emission spectrometry	Retention of n-TiO$_2$ inside the dialysis bags (*chapter 3*)
Fluorescence EEM	fluorescence excitation/emission matrix	Diffusion of DOM (fluorophores) through dialysis bags (*chapter 3*)
FT-ICR MS	Fourier transform ion cyclotron resonance mass spectrometry	Diffusion of DOM through dialysis bags (*chapter 3*)
NMR-Relaxometry	nuclear magnetic resonance-relaxometry	membrane fouling (*chapters 3 &4*)
AFM	atomic force microscopy	membrane fouling (*chapter 3*)
DO	dissolved oxygen	Bacterial activity (*chapter 3*)
DOC	dissolved organic carbon	Diffusion of DOM through dialysis bags (*chapter 3*)

Table 3: Characterization of surface waters and DOM

Abbreviations	Complete name	More information
pH meter/ thermometer	-	-(*chapters 3 & 4 & 5*)
EC	electrical conductivity	potential for surface waters to conduct electricity (*chapters 3 & 4*)
DOC	dissolved organic carbon	amount of organic matter in surface waters (*chapters 3 & 4*)
IC	ion chromatography	Measurement of the F^-, Cl^-, NO_3^-, SO_4^{2-}, PO_4^{3-}, Na^+, K^+, Ca^{2+}, and Mg^{2+} in surface waters (*chapter 3 & 4*)
ICP-OES	inductively coupled plasma-optical emission spectrometry	Measurement of the aluminum, barium, copper, iron, manganese, strontium, and zinc in surface waters (*chapter 3*)
UV-VIS	ultraviolet-visible spectrophotometry	Measurement of the degree of aromaticity (UV 254/210) in surface waters (*chapter 4*)
Fluorescence EEM	fluorescence excitation/emission matrix	Measurement of the DOM in surface waters i.e., fluorophore groups (*chapters 3 & 4*)

Table 4: Analytics to characterize n-TiO$_2$ exposed to DOM

Abbreviations	Complete name	More information
ATR-FTIR	attenuated total reflection- Fourier transform infrared Spectroscopy	Functional groups of coatings (*chapters 3 & 4 & 5*)
2D-IR	two-dimensional- infrared spectroscopy	Functional groups/ separating the effects of homogeneous and inhomogeneous dynamics (*chapter 4*)
CHNS	carbon, hydrogen, nitrogen, sulfur	Elemental analysis (*chapter 3*)
XPS	X-ray photoelectron spectroscopy	Elemental analysis, chemical environment (*chapter 4*)
ζ-Potential	Zeta potential	Charge of the nanoparticles in water (*chapter 4*)
TGA	thermogravimetric analysis	Comparison of the amount of organic and inorganic carbons (*chapter 4*)
HR-TEM	high resolution- transmission electron microscopy	Size and morphology of nanoparticles (*chapter 3*)
ToF-SIMS	Time-of-Flight Secondary Ion Mass Spectrometry	Elemental and molecular information from the surface of nanoparticles (*chapter 5*)
LDI-FT-ICR-MS	Fourier- transform ion cyclotron resonance mass spectrometry	Directly analyzes DOM after adsorption (outlook)

Table 5: Multivariate data analysis

Abbreviations	Complete name	More information
Correlation matrix	-	Correlation among variables (*chapters 4 & 5*)
PCA	principal component analysis	(*chapter 4*)
Clustering	-	Classification (*chapter 5*)
RF	random forest	Classification, the importance of variables (*chapters 4 & 5*)
EEM-PARAFAC	fluorescence excitation/emission matrix- parallel factor analysis	extract the components from mixed 3D fluorescence data (outlook)

8.2. List of Figures

8.3. List of attached files (CD)

- Dissertation thesis (PDF and Word format)
- Published articles (PDF format)
- Supporting information (PDF format)

8.4. Supporting information of Chapter 3

Table S1: Properties of the river water used for the laboratory and field experiments (May-September 2018).

Date	Conductivity (μs/cm)	pH	DOC (mg/l)	Stream flow rate (cm/s)[1]	Temp. C	Dissolved oxygen (mg/l)
Late May	271	7.2	6.1($\pm$ 0.16)[2]	-	-	-
Mid Jun	301	7.1	8.2($\pm$ 0.42)[2]	-	-	-
Mid July	280	7.1	6.1($\pm$ 0.37)[2]	-	-	-
Late July	293	7.4	6.7($\pm$ 0.21)[2]	-	-	-
Late September (field experiment)	272	7.2	6.5($\pm$ 0.15)[2]	32.3($\pm$ 7.5)[2]	21	8.79($\pm$ 1.23)[2]

[1]One meter from the river bank

[2]Standard deviation

Table S2: Total concentration of selected elements in the river water determined using ICP-OES (September 2018). LOD: limit of detection.

Elements	Concentration (μg/l)	LOD (μg/l)	Standard deviation (%)
Al	16.5	1	1.20
Ba	43.5	0.5	3.02
Ca	5246.0	1	0.35
Cu	< LOD	0.5	-
Fe	20.3	1	2.80
Ti	< LOD	0.05	-
K	509.4	2.5	0.80
Mg	1030.2	0.5	0.15
Mn	2.7	0.3	0.01
Na	3227.1	25	0.33
Sr	93.4	0.5	0.13
Zn	1.6	0.5	6.25

Table S3: Anions concentrations of the river water using ion chromatography (September 2018). LOD: limit of detection.

Anions	Concentration (mg/l)	LOD (mg/l)	Standard deviation (%)
Fluoride	0.04	0.02	4.0
Chloride	10.11	0.65	4.5
Nitrate	4.94	0.67	3.0
Phosphate	0.148	0.08	3.5
Sulphate	20.98	1.61	5.4

Figure S1: The cellulose ester dialysis bag (cylindrical design) used in this study.

Figure S2: The dialysis bags in plastic canisters deployed in the river Queich.
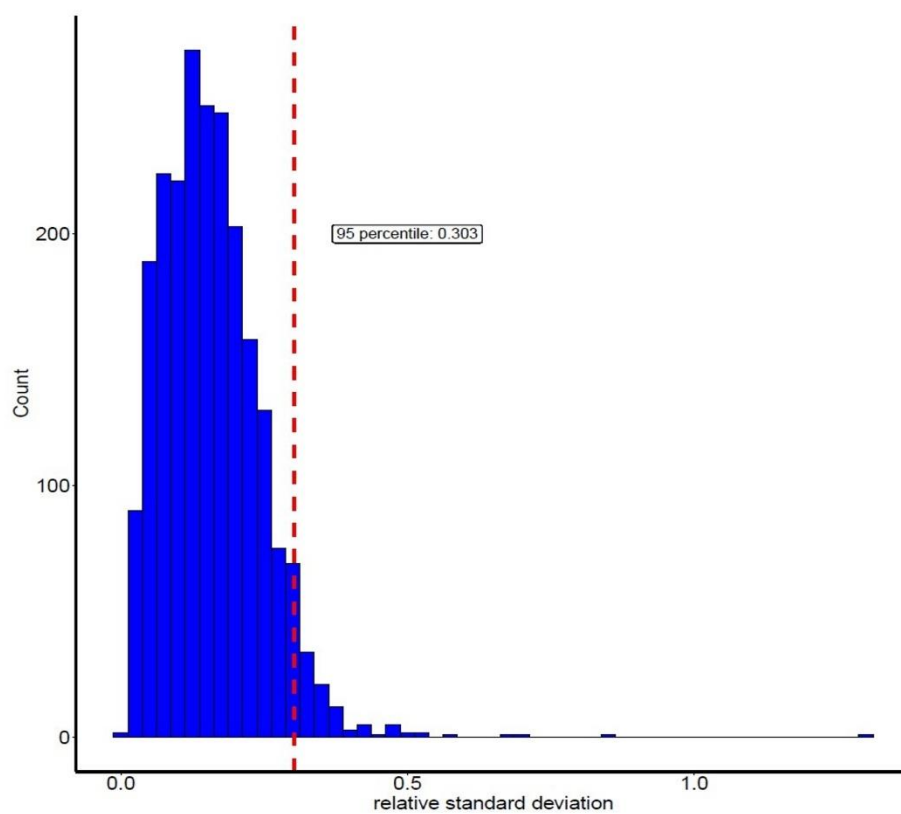
Figure S3: Assessment of the instrumental variability based on replicate measurements of SRFA ($n = 6$). Normalized intensity values were used to calculate the relative standard deviation (RSD). 95 % of the RSD values were below 0.303.
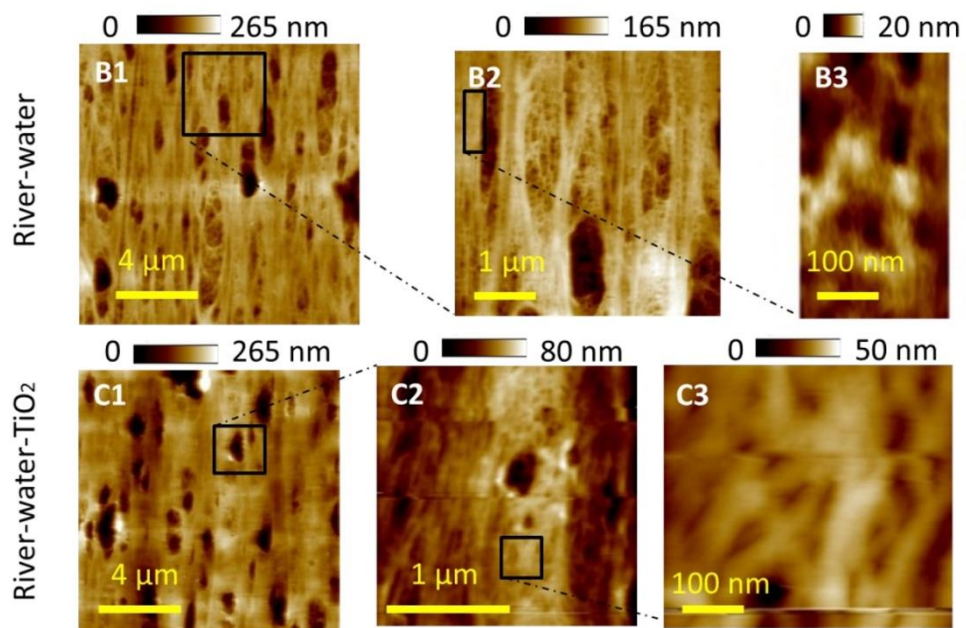
Figure S4: AFM height image of the dialysis bag in river water, and river water exposed to n-TiO$_2$.
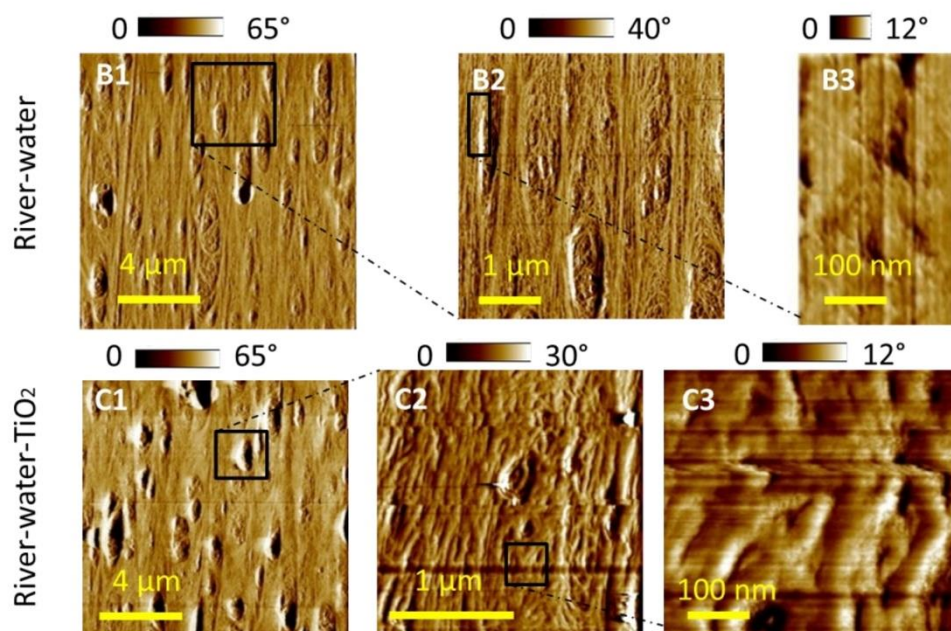

Figure S5: AFM phase image of the dialysis bag in river water, and river water exposed to n-TiO$_2$.
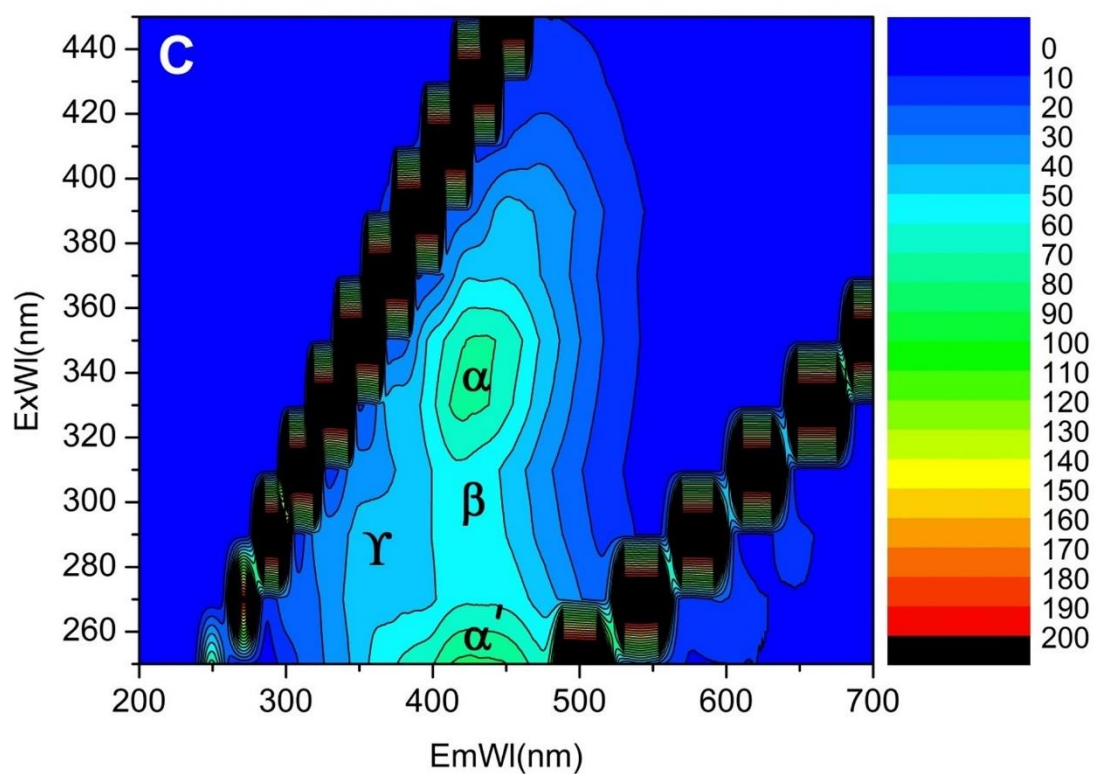
Figure S6: Fluorescence EEMs of the samples carried out in the field C) river water inside the dialysis bags with n-TiO$_2$ (the color scale depicts the intensity a.u).
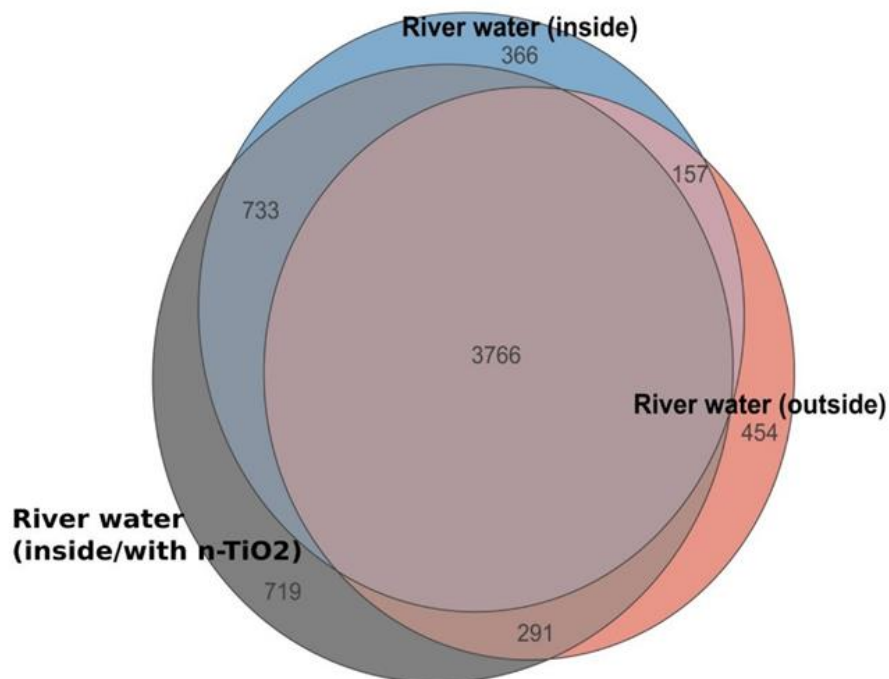

Figure S7: Euler diagram depicting the distribution of molecular formulas detected by FT-ICR-MS in all three samples (outside the dialysis bag, and inside the dialysis bag with and without n-TiO$_2$) deployed on the field.

Table S4: Major compound class distribution of all three samples deployed on the field based on the molecular formulas determined using FT-ICR-MS.

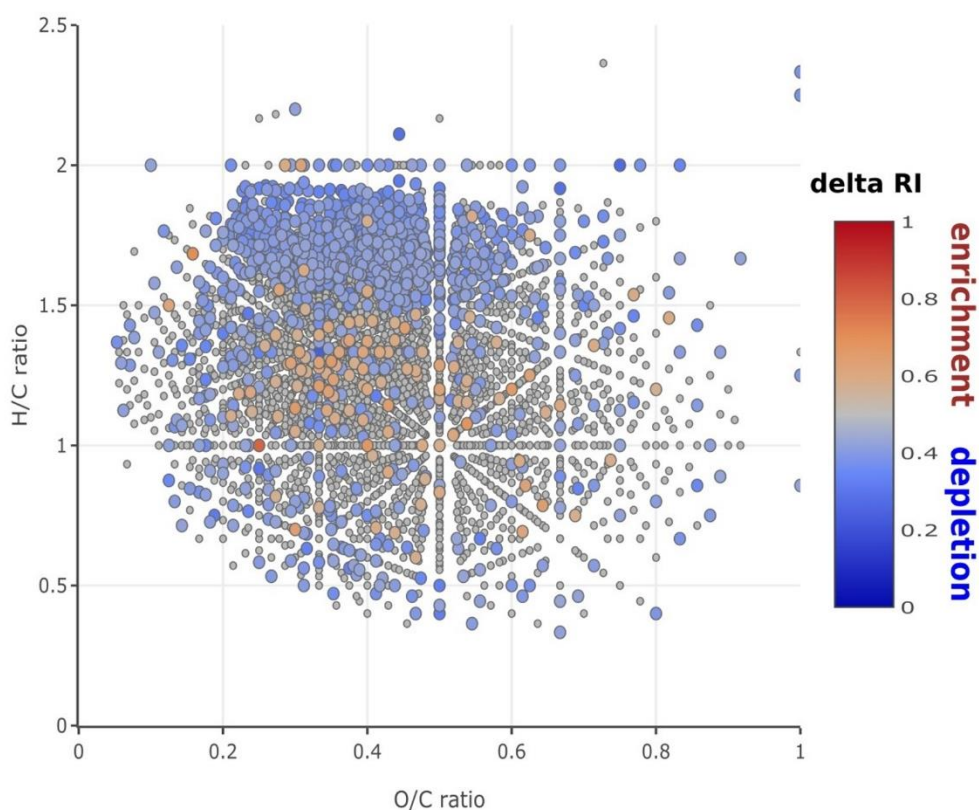| Sample	CHO	CHNO	CHOS	CHNOS	Other
River water (inside)	2677	1777	472	91	5
%	53.3	35.4	9.4	1.8	0.1
River water (outside)	2443	1565	537	116	7
%	52.3	33.5	11.5	2.5	0.1
n-TiO$_2$ (inside)	2906	1927	534	138	4
%	52.8	35.0	9.7	2.5	0.1

Figure S8: Van Krevelen diagram with intensity differences for river water inside the dialysis bags with n-TiO$_2$ vs without n-TiO$_2$. ΔRI values below 0.43 (blue) indicate the respective compound is depleted in the river water inside the dialysis bag with n-TiO$_2$ compared to without n-TiO$_2$.
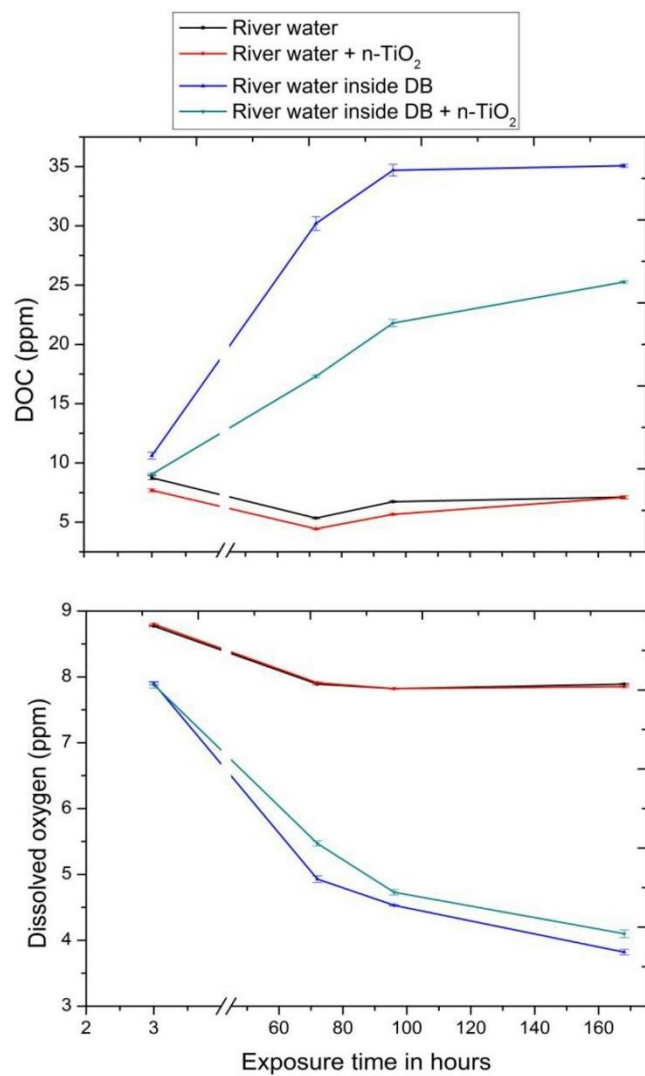
Figure S9: DOC and Dissolved oxygen of the river water inside dialysis bags (DB) with and without n-TiO$_2$, and the river water as control with and without n-TiO$_2$ at room temperature (Nov. 2019).
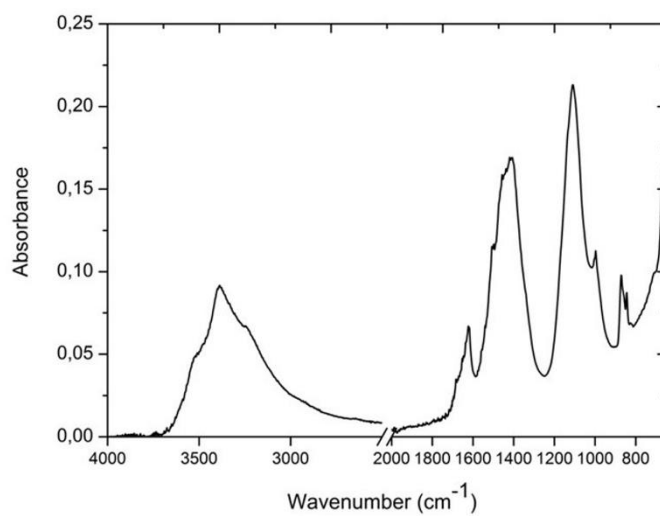

Figure S10: ATR-FTIR spectrum of the river water (freeze-dried sample).

8.5. Supporting information of Chapter 4

Table S1: The locations of surface water (SW) sites and their descriptions.

Abbr.	Site	GPS Location	Type of landscape	Description
SW1	Rehbach	49° 21' 20" N 8° 9' 19" E	urban	Is tributary of the Speyerbach river which flows through the Winziger Wassergescheid in Neustadt Weinstrasse.
SW2	Speyerbach	49°19'04.8"N 8°26'49.5"E	urban	The Speyerbach is a left tributary of the Rhine river and flows through the southern palatinate forest as splits into smaller water courses before emptying out into the Rhine.
SW3	Bischofsweiher	49°20'40.4"N 8°05'18.2"E	forest	Bischofsweier is an artificial lake dammed from inflows from the Kaltenbrunnertalbach stream and serves as a recreational fishing lake.
SW4	Kaltenbrunnertal-bach	49°20'40.4"N 8°05'18.2"E	forest	Kaltenbrunnertalbach is a stream that flows from the northern summit of Hüttenhohl and maintains its course through the southern palatinate forest before emptying into Rehbach.
SW5	Modenbach	49°16'12.4"N 8°10'58.4" E	agricultural	Modenbach is a stream, just under 30 kilometers long, and a right-hand tributary of the Speyerbach.
SW6	Neuhofener Altrhein	49°25'41.7"N 8°27'18.3"E	agricultural/ urban	This lake is primarily reserved for nature conservation with the northern beach of the lake serving as a shallow bathing area open to the public while fishing is allowed in other sections. There is a constant danger of mass development of cyanobacteria.
SW7	Kiefweiher	49°26'25.2"N 8°28'13.6"E	agricultural/ urban	Kiefweiher differs from all other lakes in the city as it is directly connected to the Rhine. This has a special effect on Rhine flood plains when the Kiefweiher overflows its banks due to outflows form the Rhine river.
SW8	Rhein	49°19'08.2"N 8°26'59.8"E	urban	The Rhine is a major European river, with its source in Switzerland. Flowing through Germany's Rhineland and the Netherlands to eventually empty into the North Sea.
SW9	Schwanenweiher	49°11'47.7"N 8°07'18.5"E	urban	It is an artificial pond located in the heart of Landau. The bank of the pond serves as a spot for recreational activities while the pond serves as a habitat for swans and fish. On Monday, July 1st, 2019, the temperature in pond increased to over 28 °C resulting in the reduction of biological oxygen demand driving most of the fish to the surface (www.pfalz-express.de).
SW10	Hainbach	49°14'09.9"N 8°04'25.3"E	Forest/agric ultural	It is a tributary of the Speyerbach that runs through palatinate forest and serves as a natural irrigation for the vineyards and agricultural fields.

Table S2: The average of surface water parameters between the first and last day of exposure for spring and summer samples.[1]

Site	pH	Temp. (°C)	EC (µS/cm)	DOC (mg/L)	F⁻ (mg/L)	Cl⁻ (mg/L)	NO₃⁻ (mg/L)	SO₄²⁻ (mg/L)	PO₄³⁻ (mg/L)[2]	Na⁺ (mg/L)	K⁺ (mg/L)	Ca²⁺ (mg/L)	Mg²⁺ (mg/L)	Flu. fulvic/humic acid[3]	UV 254/210	Flu. Protein[4]
SW1-Sp.	7.9	11.2	147.5	2.3	0.04	10.6	4	14.4	0.2	9.1	4	14.9	4.1	0.9	0.03	1
SW1-Su.	7.8	13.8	154.0	8.8	0.01	6.0	1.9	7.3	0.2	8.4	3.4	15.7	3.3	0.6	0.04	0
SW2-Sp.	8	13.1	347.5	3.8	0.04	25.3	6.7	27.8	0.2	19.5	6.6	24.9	5.8	1.0	0.05	1
SW2-Su.	7.6	15.3	323.5	4.5	0.03	8.8	2.7	6.8	0.2	21.2	6.4	20.3	3.7	0.7	0.05	1
SW3-Sp.	7.4	11.1	122.0	3.0	0.05	9.2	4.3	14.2	<LOD	5.9	2.5	10.4	4.6	0.7	0.11	0
SW3-Su.	6.8	14.5	79.0	10.5	0.05	3.3	0.5	4.1	<LOD	2.3	1.2	5.3	1.1	0.5	0.29	0
SW4-Sp.	7.4	11.2	123.5	3.9	0.05	12.0	2.8	13.6	<LOD	5.7	2.7	9.4	4.0	0.6	0.10	0
SW4-Su.	6.8	14.6	84.0	6.2	0.07	3.1	0.4	3.5	<LOD	5	3	9.9	3.2	0.5	0.30	0
SW5-Sp.	8.1	11.3	357.0	3.1	0.07	11.6	5.2	21.6	<LOD	8.1	2.9	42.8	12.8	0.8	0.04	1
SW5-Su.	7.8	16.3	444.5	11.6	0.08	9.3	2.8	14.1	<LOD	6	1.8	42.8	9.4	0.5	0.05	0
SW6-Sp.	7.9	16.4	748.0	9.7	0.06	49.0	2.8	180	<LOD	24.3	6.7	86.5	21.3	0.7	0.07	1
SW6-Su.	7.9	21.6	817.0	13.6	0.08	20.1	0.3	40.4	<LOD	24.9	7	102.1	20.1	0.5	0.29	1
SW7-Sp.	8.4	16.2	338.0	3.5	0.07	20.3	4.3	27.6	<LOD	13.6	2.5	46.7	8.6	0.8	0.06	1
SW8-Sp.	8.2	13.6	349.5	2.9	0.07	19.6	5.4	25.8	<LOD	13.8	2.4	48.8	8.5	0.8	0.05	1
SW8-Su.	7.8	19.7	329.0	12.5	0.08	4.6	1.4	7.5	<LOD	10.5	2.1	34.5	6.9	0.5	0.05	0
SW9-Sp.	9.1	14.8	495.0	17.1	0.07	59.5	1.6	46.2	<LOD	38.9	10	30.5	11.9	0.9	0.19	1
SW9-Su.	8.6	23.4	852.5	19.3	0.09	133.2	1.8	30.8	0.2	62.3	15.5	63.1	18.8	0.6	0.17	1
SW10-Su.	7.5	16.4	119.5	5.6	0.07	4.1	1.7	6.6	0.1	3.5	2.4	16.2	3.8	1.0	0.15	0

[1] Sp. = spring (18.04.2019-22.04.2019) and Su. = summer (12.09.2019-16.09.2019). The data for SW10-Sp. and SW7-Su. are not available because the samples could not be retrieved after exposure.

[2] LOD (limit of detection) of phosphate = 0.08 mg/L.

[3] Fluorescence intensity ratio of fulvic/humic acid (fulvic: fluorescence intensity measured at Ex/Em ~ 340/430 and humic: fluorescence intensity measured at Ex/Em ~ 250/430).

[4] Tryptophane-like proteins in SWs were shown as "Flu. Protein" (on fluorescence map: Ex/Em ~ 270/330). Presence of "Fluo. Protein" = 1, Absence of "Flu. Protein" = 0.

Table S2-1: Calculations[1] of saturation index (SI) based on the parameters of Table S2.

Site	Ionic Strength	Saturation index.[2] (calcite)[3]
SW1-Sp.	2.06e-03	-0.944
SW1-Su.	1.74e-03	-1.083
SW2-Sp.	3.47e-03	-0.532
SW2-Su.	2.26e-03	-1.366
SW3-Sp.	1.58e-03	-2.089
SW3-Su.	5.74e-04	-3.512
SW4-Sp.	1.49e-03	-2.130
SW4-Su.	1.04e-03	-3.254
SW5-Sp.	4.38e-03	-0.124
SW5-Su.	3.64e-03	-0.659
SW6-Sp.	9.97e-03	-0.268
SW6-Su.	8.33e-03	-0.093
SW7-Sp.	4.95e-03	0.545
SW8-Sp.	4.72e-03	0.149
SW8-Su.	2.94e-03	-0.708
SW9-Sp.	1.03e-02	1.553
SW9-Su.	9.73e-03	1.076
SW10-Su.	1.53e-03	-1.638

[1] Calculations were performed using "visual MINTEQ 3.1" considering the atmospheric pressure of 0.00038 atm for CO_2.
[2] Saturation Index (SI) = log IAP – log K_{sp} (IAP: Ion activity product and K_{sp}: Solubility Product)
SI > 0: oversaturation (precipitation)
SI = 0: apparent equilibrium
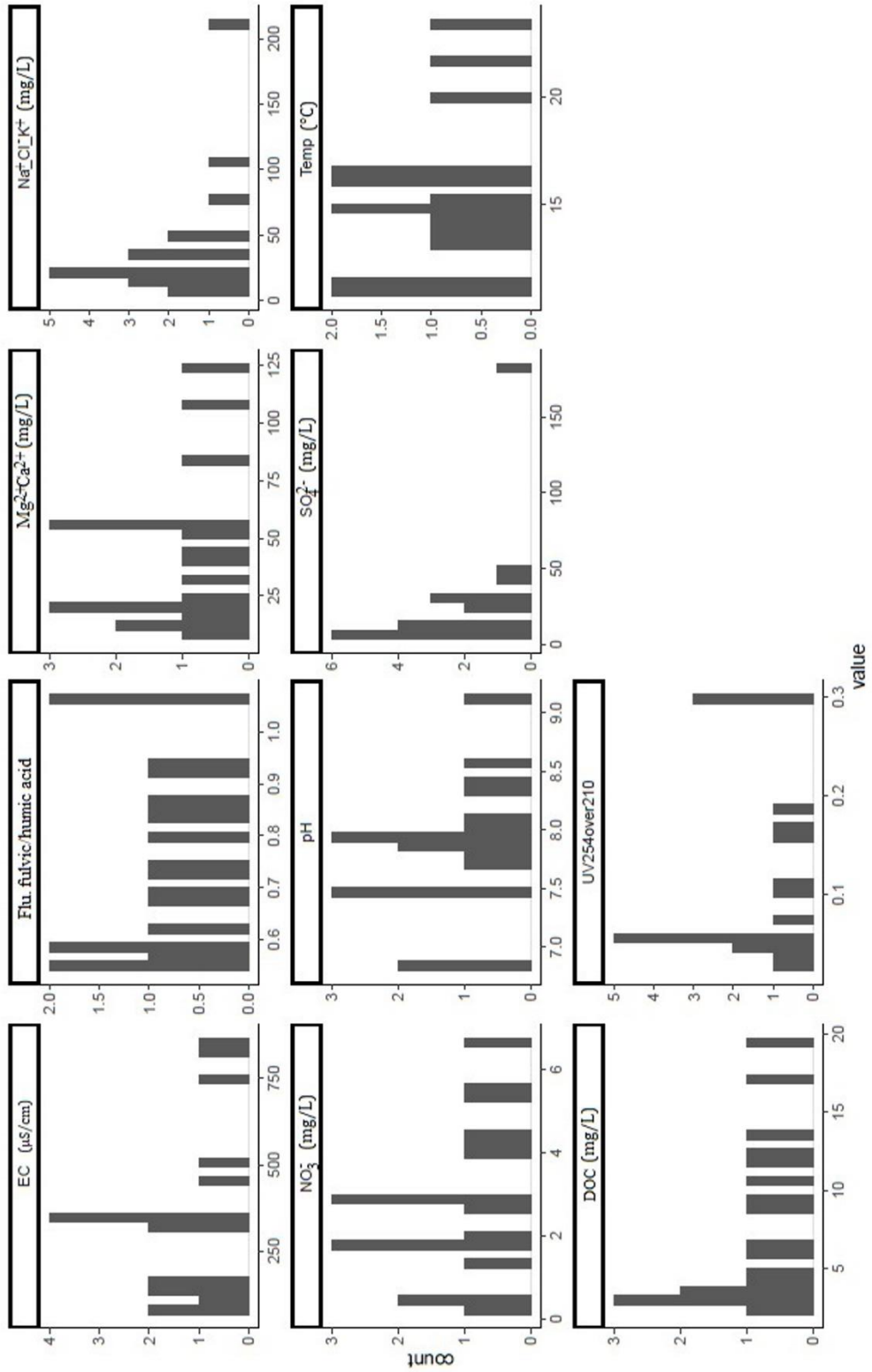SI < 0: undersaturation
[3] Calcite: $CaCO_3$

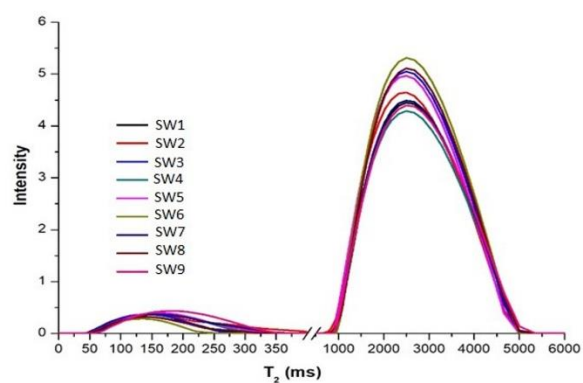**Figure S1:** Density plots of the physiochemical parameters of the surface waters.

Figure S2: T_2 distribution comparison of dialysis bags containing n-TiO$_2$ exposed to surface waters SW1-SW9 during spring obtained using ^{1}H-NMR relaxometry. Sample SW10 was not retrieved.
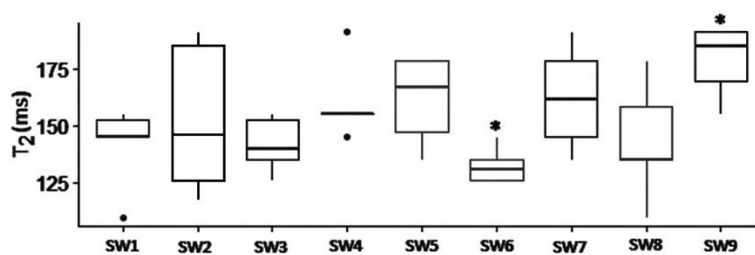

Figure S3: Box plots showing variances in T_2-distribution mode (small pores) within each six replicates in spring experiment. Sample SW10 was not retrieved. Asterisks show the samples with significant difference based on a Tukey test.
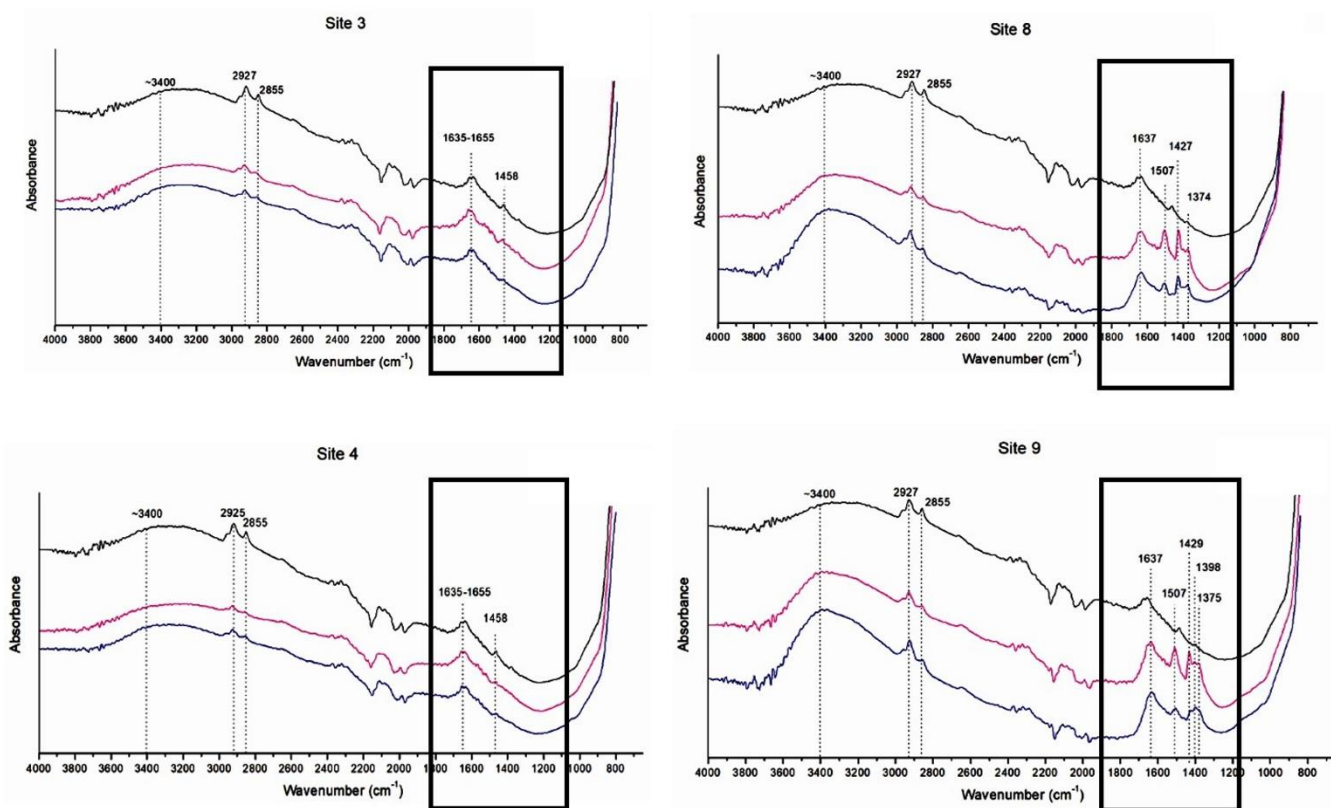
Figure S4: Representative ATR-FTIR spectra of the SW3, SW4, SW8, and SW9 in summer experiments. Black spectra: n-TiO$_2$, Red spectra: n-TiO$_2$/SWs, Blue spectra: n-TiO$_2$/SWs rinsed with pure water.

Table S3: Presence or absence of new ATR-FTIR bands on n-TiO$_2$ after exposure to SWs (n-TiO$_2$/SWs).

Site	Season	IR-wide1375-1398	IR-sharp-1430	IR-1500
SW1	Spring	X	-	-
	Summer	-	-	-
SW2	Spring	X	-	X
	Summer	X	-	-
SW3	Spring	-	-	-
	Summer	-	-	-
SW4	Spring	-	-	-
	Summer	-	-	-
SW5	Spring	X	-	X
	Summer	X	X	X
SW6	Spring	X	-	X
	Summer	X	X	X
SW7	Spring	X	X	X
	Summer	NA	NA	NA
SW8	Spring	X	X	X
	Summer	X	X	X
SW9	Spring	X	X	X
	Summer	X	X	X
SW10	Spring	NA	NA	NA
	Summer	X	-	-

X: presence of assigned ATR-FTIR band.

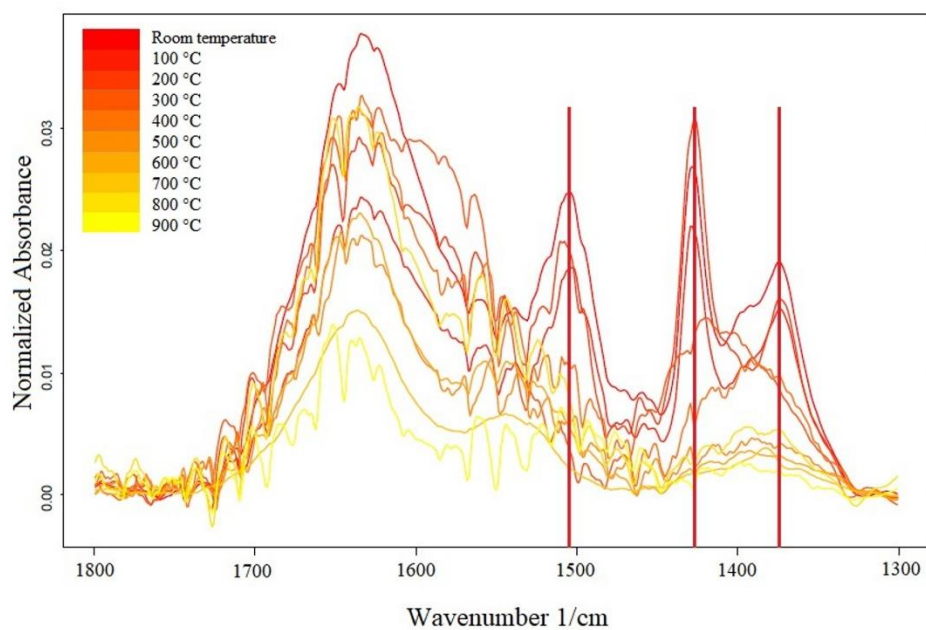NA: lost sample/ samples could not be retrieved after exposure.

Figure S5: ATR-FTIR spectra of TiO$_2$/SW8 calcined stepwise from room temperature to 900 °C.
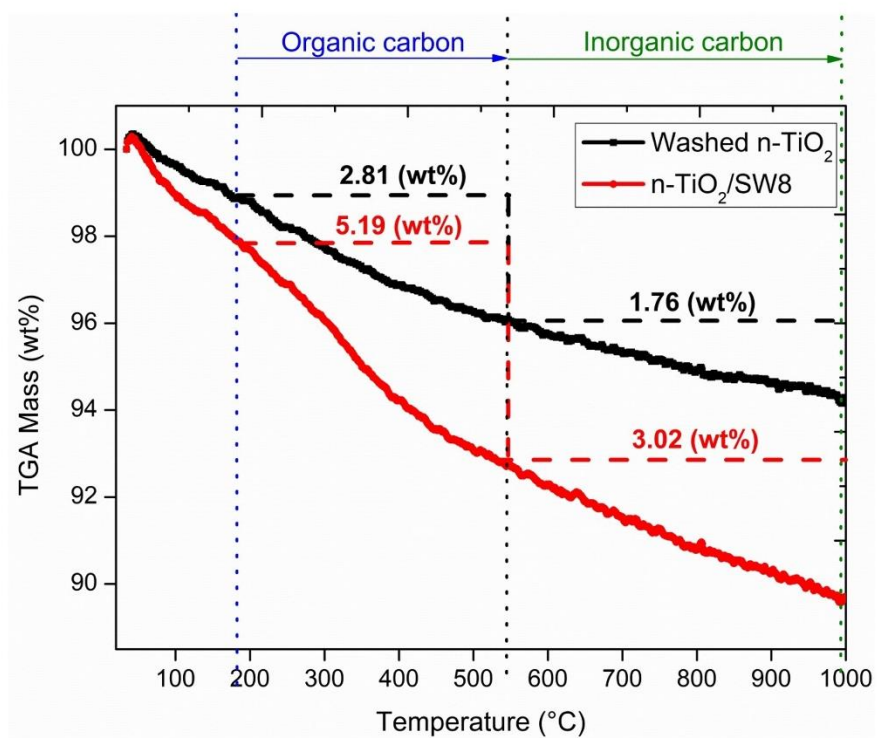
Figure S6: TGA curves for washed n-TiO$_2$ (control sample) and n-TiO$_2$/SW8.

Table S4: Atomic percentage of the elements present on-TiO₂/SWs samples in summer experiment obtained from XPS analysis.

Photoelectron line	Binding Energy (eV)	SW1 Atomic %	SW2 Atomic %	SW3 Atomic %	SW4 Atomic %	SW5 Atomic %	SW6 Atomic %	SW8 Atomic %	SW9 Atomic %	SW10 Atomic %	n-TiO2[1] Atomic %	Assigned bonds or functions
P 2p$_{3/2}$	133.6	0.2	0.1	-	-	0.2	-	0.1	0.0	0.1	-	PO_4^{3-}
S 2p$_{3/2}$	168.9	0.7	0.6	0.4	0.4	0.6	0.8	0.4	0.4	0.4	-	SO_4^{2-}
C 1s	285.0	24.4	26.2	26.5	26.9	26.5	27.7	28.5	27.0	26.9	19.5	C-C and C-H
C 1s	286.7	2.5	2.4	2.4	2.3	2.6	2.4	2.0	2.6	2.5	1.7	C-O
C 1s	288.6	1.4	1.7	1.8	1.4	1.9	1.9	1.5	1.7	1.8	1.8	O-C=O
C 1s	289.7	0.4	0.5	0.2	0.1	0.9	0.9	1.0	1.0	0.4	-	CO_3^{2-}
C total		*26.9*	*30.8*	*30.8*	*33.2*	*33.9*	*32.7*	*33.2*	*32.3*	*31.8*	*23.0*	
Ca 2p$_{3/2}$	347.6	0.4	0.8	0.2	0.2	1.5	1.5	1.4	1.5	0.6	-	Ca^{2+}
Mg 1s	1304.4	0.1	0.2	0.1	-	0.3	0.7	0.2	0.3	0.2	-	Mg^{2+}
Ti 2p$_{3/2}$	458.9	19.7	18.9	20.1	19.8	18.1	17.7	18.0	18.4	19.1	23.8	Titanium in TiO_2
O 1s	530.1	39.4	38.0	40.5	39.7	35.5	34.6	36.6	36.8	38.1	47.4	Oxygen in TiO_2
O 1s	531.9	10.0	9.9	7.3	8.0	11.4	11.2	9.6	9.8	9.4	5.6	Oxygen in C-O, O-C=O, CO_3^{2-}, PO_4^{3-}, SO_4^{2-}

[1] washed n-TiO₂ (control sample) before exposure to surface waters.

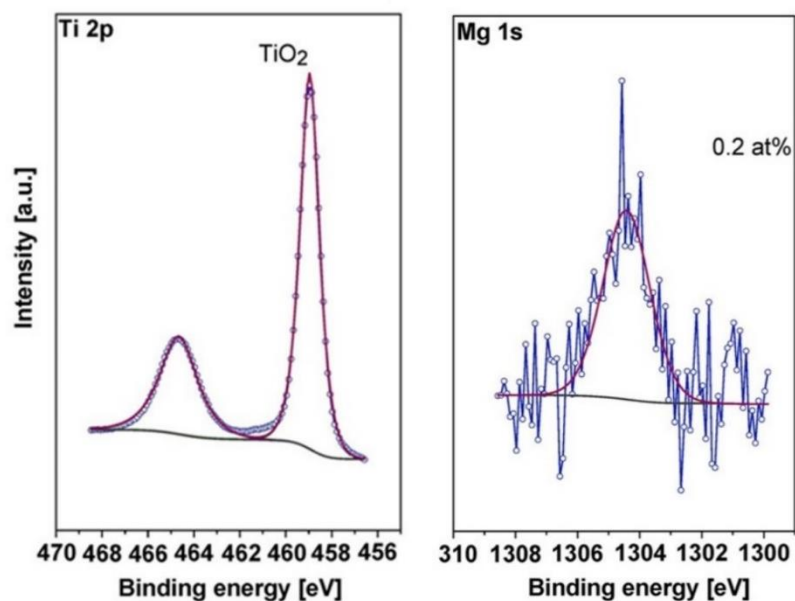The data for SW7 is not available because the samples could not be retrieved after exposure.

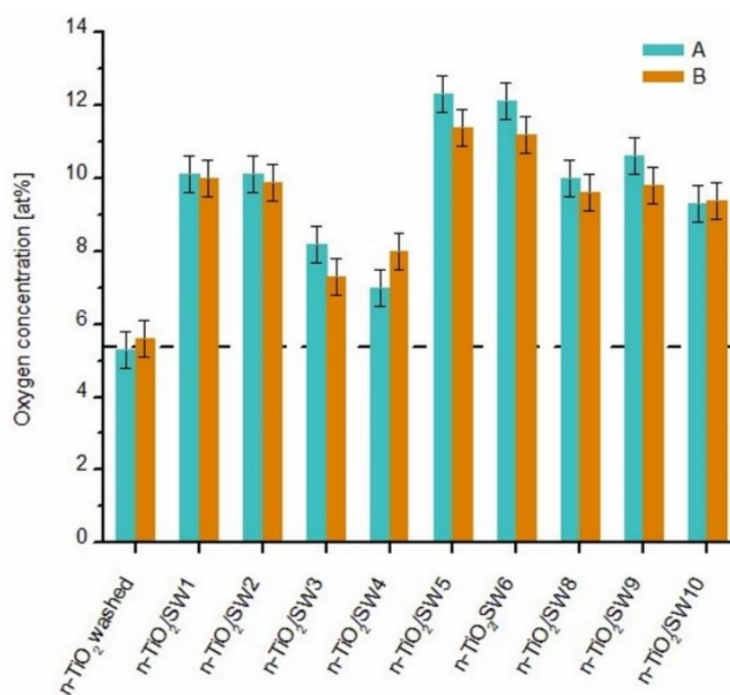**Figure S7**: Illustrative Ti 2p and Mg 1s XPS peaks, baseline and fittings for n-TiO₂/SW8.

Figure S8: Comparison of oxygen content of n-TiO₂ exposed to SWs (n-TiO₂/SWs) in summer experiment. A) expected oxygen% in oxygen containing compounds calculated from C—O, O—C=O, and CO_3^{2-} (C 1s), SO_4^{2-} (S2p$_{3/2}$), and PO_4^{3-} (P2p$_{3/2}$), B) oxygen% measured for O 1s at 531.9 eV. Sample SW7 could not be recovered. (The dashed line depicts the oxygen concentration (531.9 eV) in washed n-TiO₂).
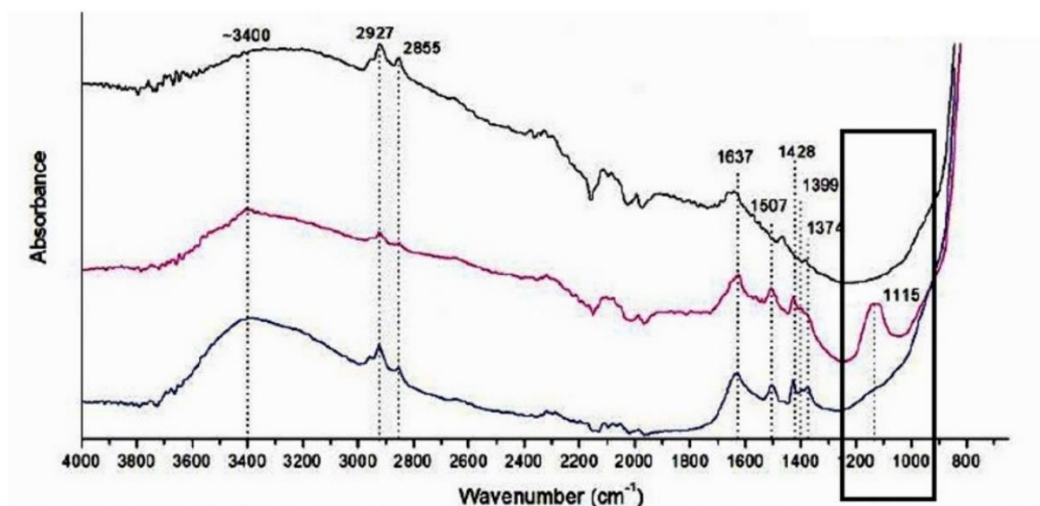
Figure S9: Representative ATR-FTIR spectra of n-TiO$_2$ exposed to SW6 in summer experiment. Black spectra: n-TiO$_2$, Red spectra: n-TiO$_2$/SW6, Blue spectra: n-TiO$_2$/SW6 rinsed with pure water.
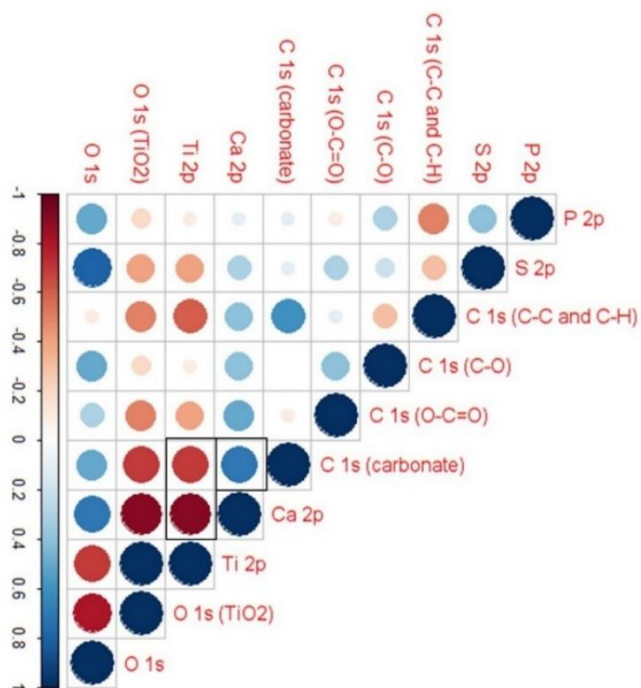

Figure S10: Correlation matrix among the elements and functional groups (analyzed by XPS) on the surface of n-TiO$_2$ exposed to surface waters (SW1-SW10). The color scale on the left denotes the correlation coefficient. The important correlations are framed.

Table S5: Zeta potential of n-TiO$_2$/SWs samples in the summer experiment.[1]

TiO$_2$ nanoparticles exposed to surface waters	pH[2]	Zeta Potential (mV)
n-TiO$_2$/SW1	6.8	-13.25 ± 1.02
n-TiO$_2$/SW2	7.1	-27.18 ± 0.85
n-TiO$_2$/SW3	6.5	-8.11 ± 0.57
n-TiO$_2$/SW4	6.8	-11.53 ± 3.43
n-TiO$_2$/SW5	8.2	-45.86 ± 1.73
n-TiO$_2$/SW6	8.2	-23.11 ± 0.92
n-TiO$_2$/SW8	8.0	-26.18 ± 1.02
n-TiO$_2$/SW9	8.0	-25.15 ± 0.58
n-TiO$_2$/SW10	7.2	-21.07 ± 1.67
Washed n-TiO$_2$	6.5	-6.04 ± 1.25

[1] The zeta potential was measured at 24 °C with ionic strength of 0.01 M.

[2] The pHs of the samples are around the neutral pH, so they can be comparable.
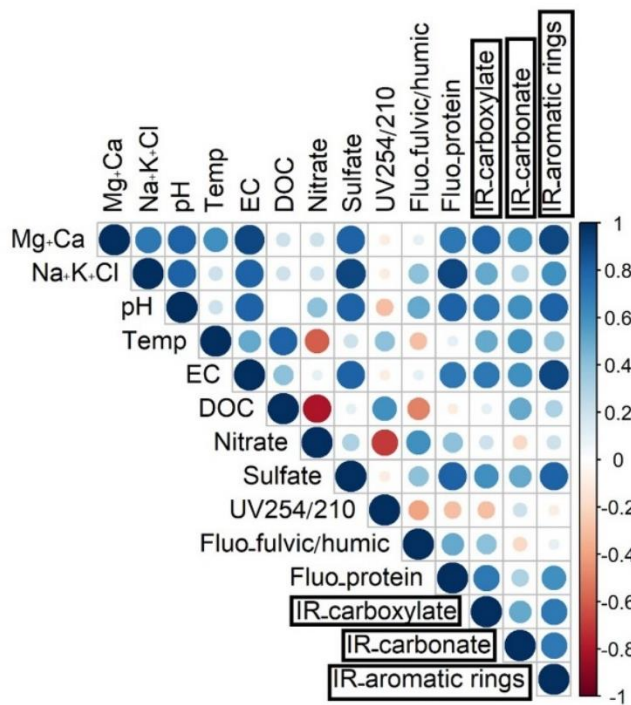
Spearman's correlation matrix:

Figure S11: Correlation matrix among physicochemical parameters of SWs and functional groups appeared on nanoparticles after exposure to SWs. The color scale on the left shows (r) correlation coefficient. EC: electrical conductivity; DOC: dissolved organic carbon; Flu. Protein: presence of a protein's fluorescence peak at Ex/Em ~ 270/330; Flu. fulvic/humic acid: the ratio of fluorescence intensity at Ex/Em ~ 340/430 to Ex/Em ~ 250/430. The functional groups assigned for IR bands are framed.
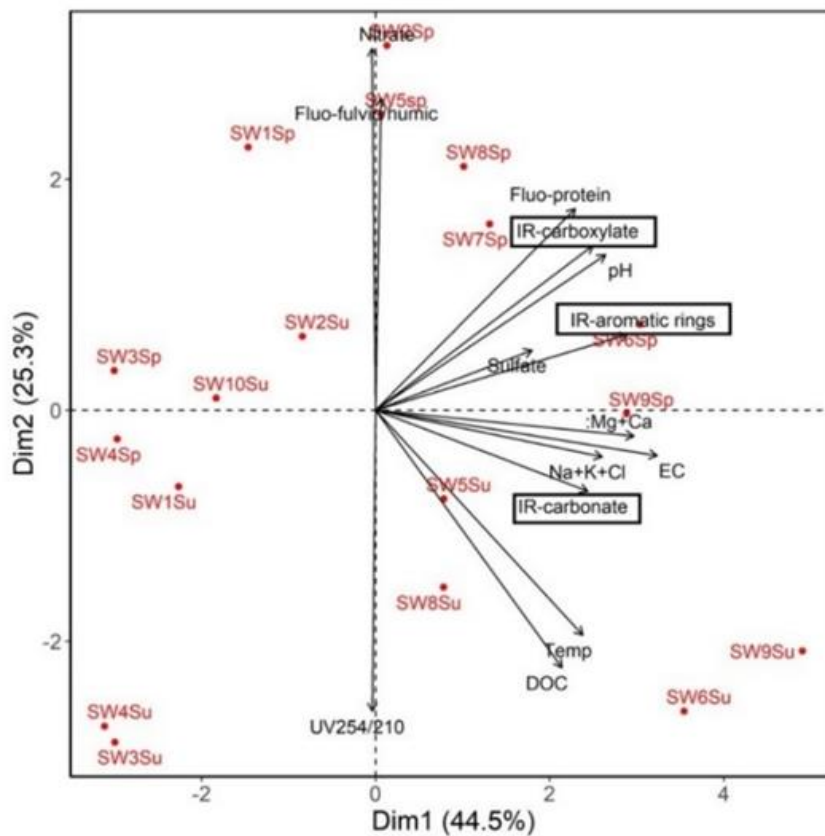
Figure S12: PCA biplot of individuals and variables. The biplot shows the PCA scores of variables (SWs physicochemical parameters) as vectors in black, and individuals i.e., samples in red. Spring and summer experiments are depicted by sp. and su., respectively. EC: electrical conductivity; DOC: dissolved organic carbon; Flu. Protein: presence of a protein's fluorescence peak at Ex/Em ~ 270/330; Flu. fulvic/humic acid: the ratio of fluorescence intensity at Ex/Em ~ 340/430 to Ex/Em ~ 250/430. The functional groups assigned for IR bands are framed.
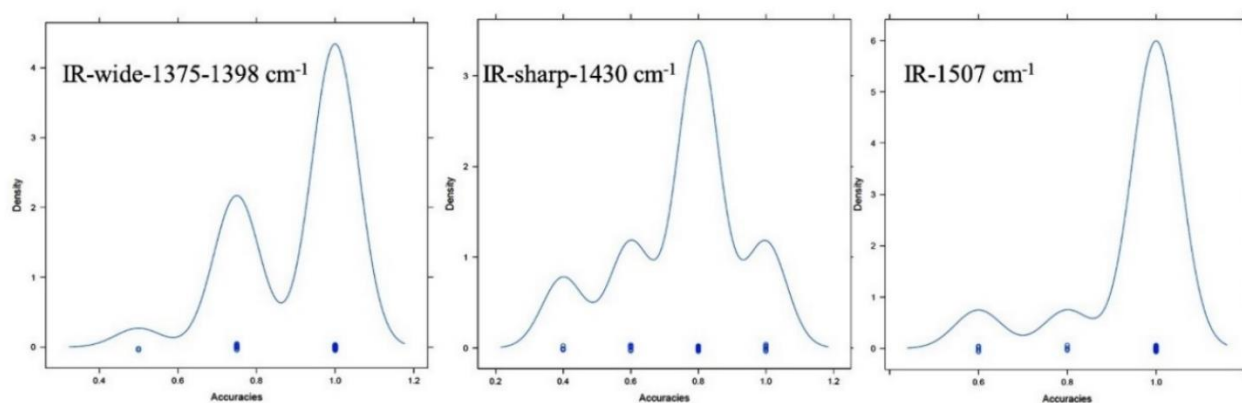

Figure S13: Density plots of the accuracy of the RF-models (50 models from 50 different initial data partitioning) for ATR-FTIR bands of n-TiO$_2$/SWs.

8.6. Supporting information of Chapter 5

Table S1. ID numbers, and SPF of the 10 studied sunscreens containing n-TiO$_2$. The detailed specification of each sunscreen can be found elsewhere [1].

Number	Trade Name[1]	Particle Shape [1]	Size (nm)[2] [1]	Isoelectric Point [1]	Surface Coating[3] [1]	n-TiO$_2$ content (mg)[4]
1	Rewe Feuchtigkeits-Sonnenspray/ SPF (30)	Spherical, irregular	23.2 ± 1.2	2.6	PDMS	1.97 ± 0.14
2	Rewe Feuchtigkeits-Sonnencreme/ SPF (50)	Spherical and angular	28.0 ± 1.0	2.2	PDMS	2.23 ± 0.26
3	Real,-Quality Sonnenmilch/ SPF (30)	Ellipsoidal and angular	35.5 ± 2.0	1.7	PDMS	2.42 ± 0.18
4	Real,- Quality Sonnencreme/ SPF (30)	Spherical	19.3 ± 0.8	1.9	PDMS	1.66 ± 0.20
5	Biotherm Lait Solaire/ SPF (50)	Elongated	24.8 ± 0.8	1.9	PDMS	1.79 ± 0.09
6	Nivea Sun Pflegende Sonnenmilch/ SPF (50)	Spherical	34.3 ± 0.6	<1.8	SiO$_2$	2.29 ± 0.35
7	Sundance Sonnenmilch/ SPF (50)	Ellipsoidal	30.8 ± 1.0	<1.8	PDMS	2.21 ± 0.33
8	Garnier Ambre Solaire Resisto Sonnenschutz-Milch/ SPF (50)	Elongated, spherical and ellipsoidal	22.3 ± 0.8	2.1	PDMS	2.63 ± 0.04
9	Alverde Sonnencreme Jojoba/ SPF (30)	Spherical, angular and elongated	35.6 ± 0.6	4.5	Al$_2$O$_3$	3.38 ± 0.18
10	Baby sebamed Sonnenschutzlotion/ SPF (50)	Ellipsoidal and spherical	27.4 ± 1.7	3.1	Al$_2$O$_3$+SiO$_2$	2.33 ± 0.18

[1] based on the information written on their packages.[2] average hydrodynamic diameter (nm)[3] proposed surface coatings analyzed by ToF-SIMS.[4] n-TiO$_2$ content extracted from 50 mg sunscreen (calculated based on the n-TiO$_2$ content in the initial sunscreen and the corresponding recoveries after the extraction **[1]**).

Table S2. Summary of random forest models performances.

	S3[1]	S4[2]	S9[3]
Accuracy on test set (in %)	100	100	100
95% confidence interval in %	0.8456–1	0.8456–1	0.8456–1
mtry	85	50	2
Node size	1	1	1
Sample size	0.63	0.63	0.63
Out of bag error	0.04	0.00	0.00

[1] n-TiO$_2$ ⊂ sunscreen (3) exposed to fulvic acids.[2] n-TiO$_2$ ⊂ sunscreen (4) exposed to fulvic acids.[3] n-TiO$_2$ ⊂ sunscreen (9) exposed to fulvic acids.
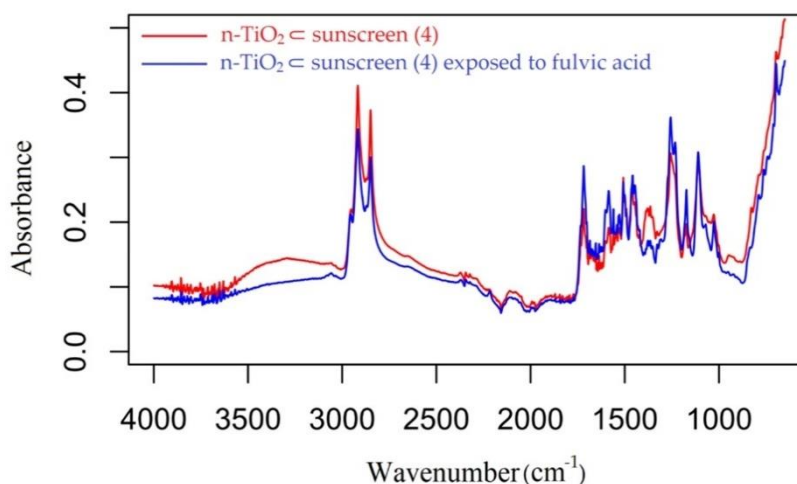

Figure S1. (a) Representative ATR-FTIR spectra of the n-TiO$_2$ ⊂ sunscreen (4) before and after exposure to fulvic acids. No presence of new bands or band shift is seen on the surface of n-TiO$_2$ ⊂ sunscreen (4) after exposure to fulvic acids (since the analysis was performed qualitatively, the changes in absorbance are not interpretable).
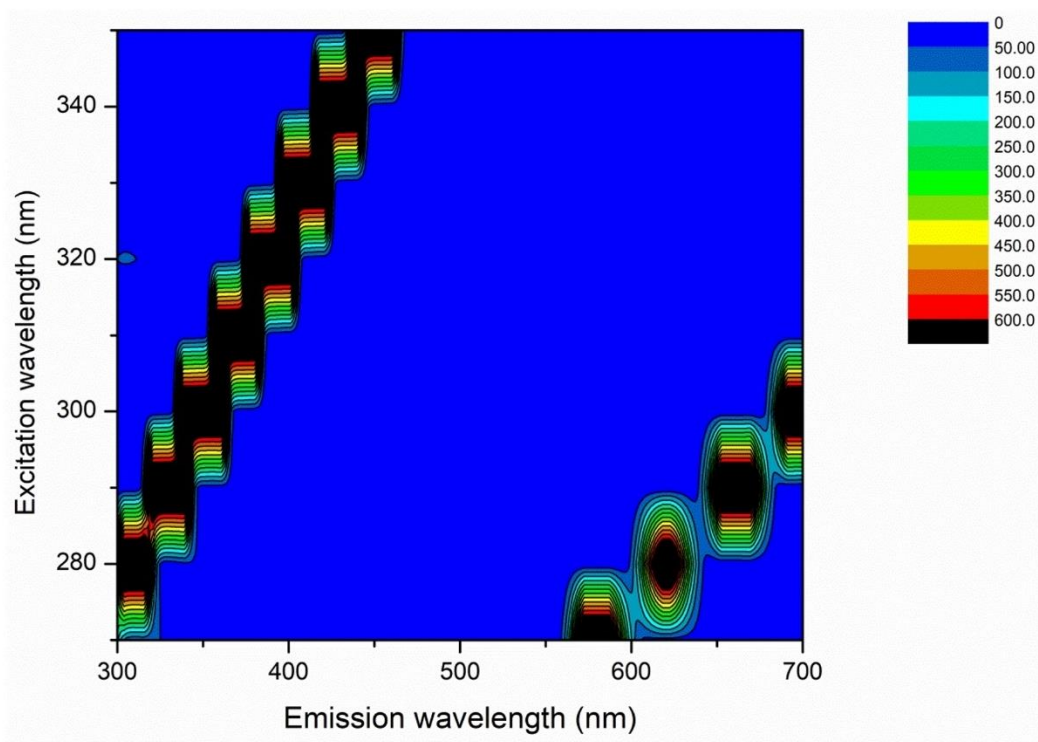
Figure S1. (b). Three-dimensional excitation-emission-matrix (EEM) fluorescence spectroscopy of n-TiO$_2$ ⊂ sunscreen(4) exposed to fulvic acid. No peaks depicting the presence of fulvic acids (excitation/emission ~ 310/450 nm) [2] can be detected on the nanoparticles (The color scale depicts the intensity, and the black lines depict fluorescence scattering).
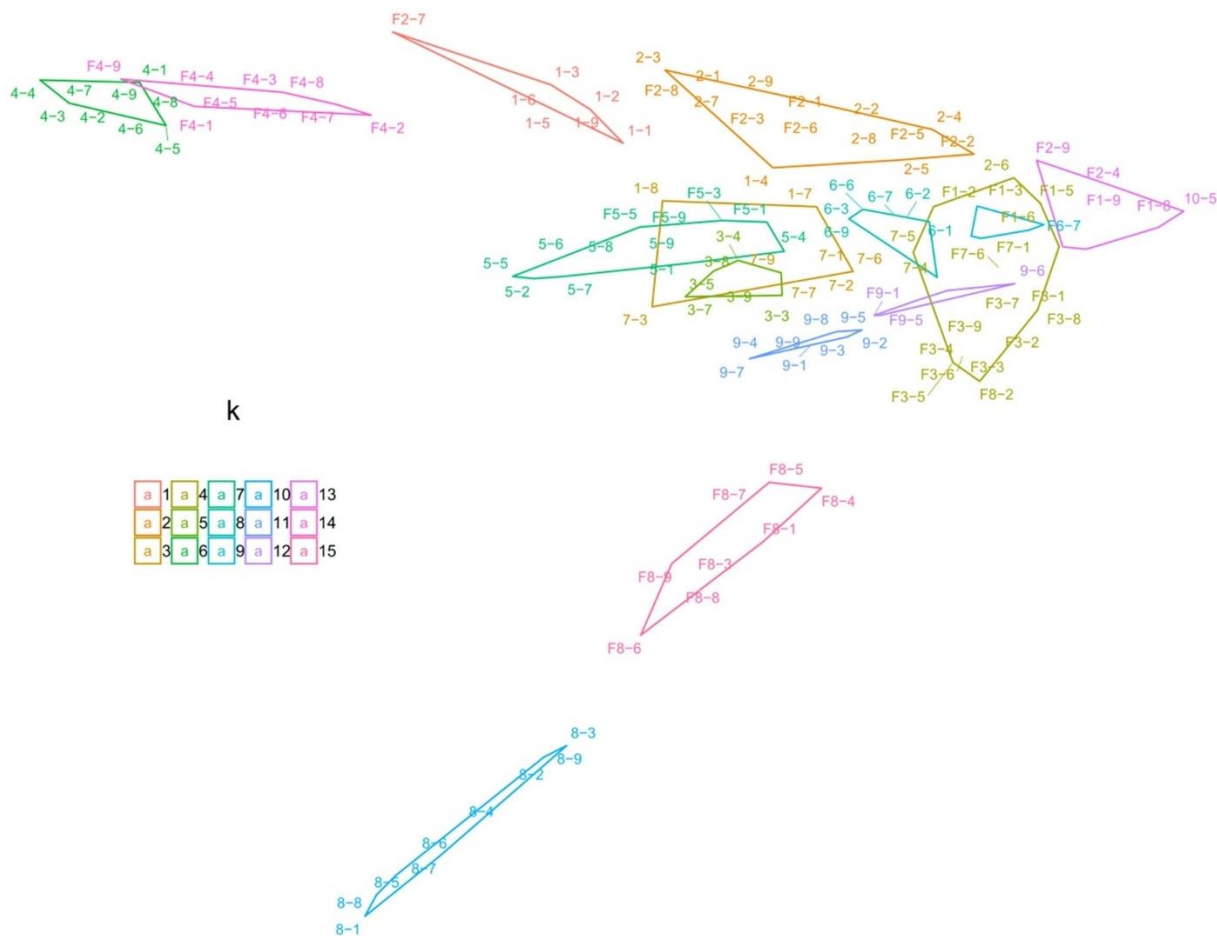
Figure S2. K-mean clustering of n-TiO$_2$ $\subset$ sunscreen samples for 10 different sunscreens before (X-Y) and after (FX-Y) exposure to fulvic acid where X and Y depict the sunscreen's ID and the number of replicates, respectively. F represents the exposure to fulvic acids. K depicts the numbers of the clusters. Here, the optimized total number of clusters is 16. It has to be noted that the projection of the clusters on the 2D plane shown above is based on PCA, the overlapping of the clusters can be due to their projection in 2D. Since our data do not satisfy requirements for PCA (no linear gradient and skewed data), interpretation in terms of distances on the above graph should be avoided. Therefore, the projection on the plane formed by the two principal components is for visualization purposes only.
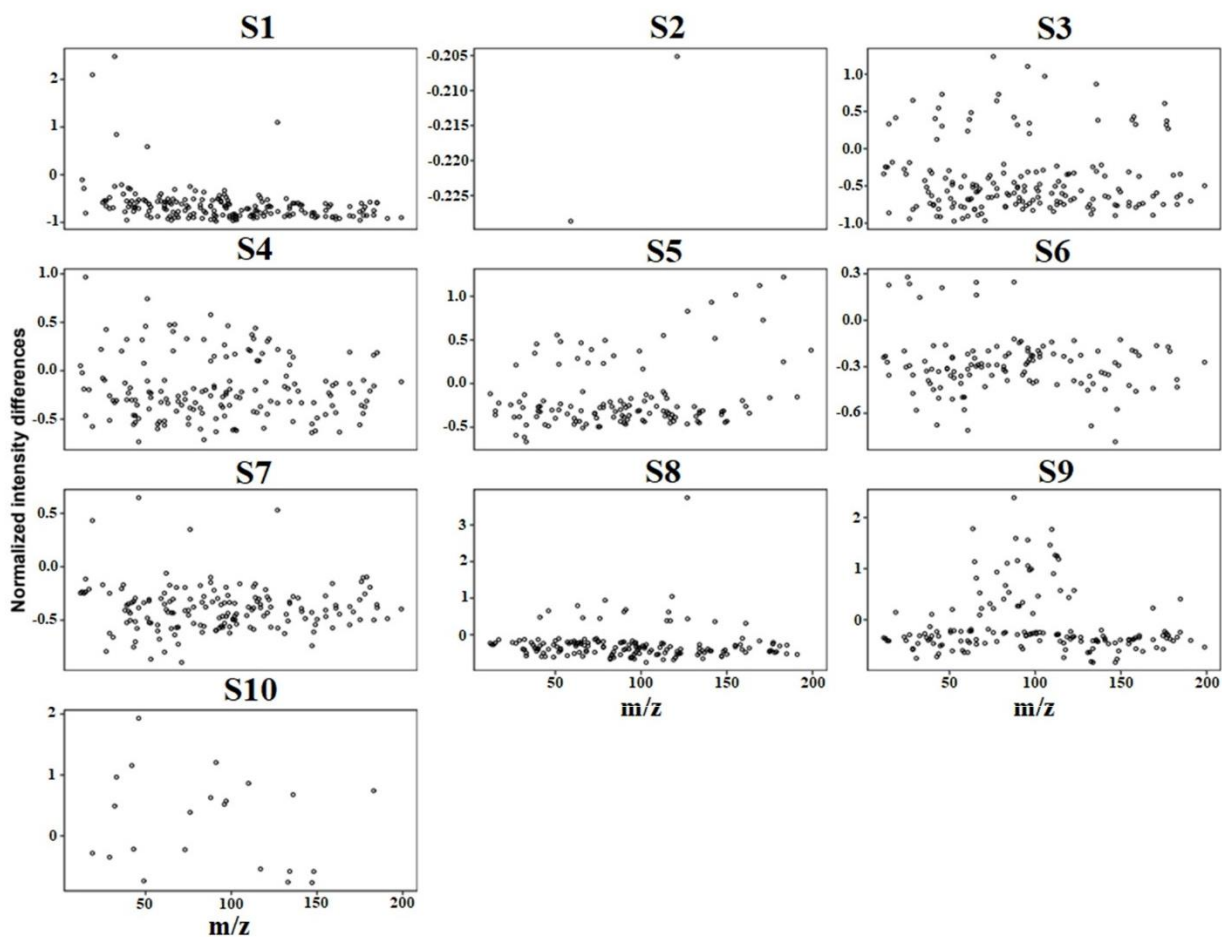
Figure S3. Significant (t-test 95% confidence) differences in the normalized intensities (negative polarity) averaged over 9 replicates for all masses detected using ToF-SIMS for n-TiO$_2$⊂ sunscreen samples before and after exposure to fulvic acids.

Table S3. The number of common masses[a] of n-TiO$_2$⊂ sunscreen samples with increased-signal intensities after exposure to fulvic acids (X depicts the sunscreen's ID).

X	1	2	3	4	5	6	7	8	9	10
1	5									
2	0	0								
3	1	0	29							
4	1	0	1	40						
5	0	0	2	2	25					
6	1	0	2	5	0	8				
7	2	0	3	0	0	0	4			
8	1	0	4	5	4	1	3	16		
9	1	0	1	17[b]	0	2	1	3	39	
10	1	0	5	4	1	2	2	3	2	12

[a] Calculated from FX-X > 0 i.e. differences of signal intensities of n-TiO$_2$ from the corresponding signal intensities of the same nanoparticles exposed to fulvic acids (9 replicates for each ToF-SIMS measurement). [b] The highest number of common masses (increased-intensity signals) is seen between samples 4 and 9 (17 common mass).
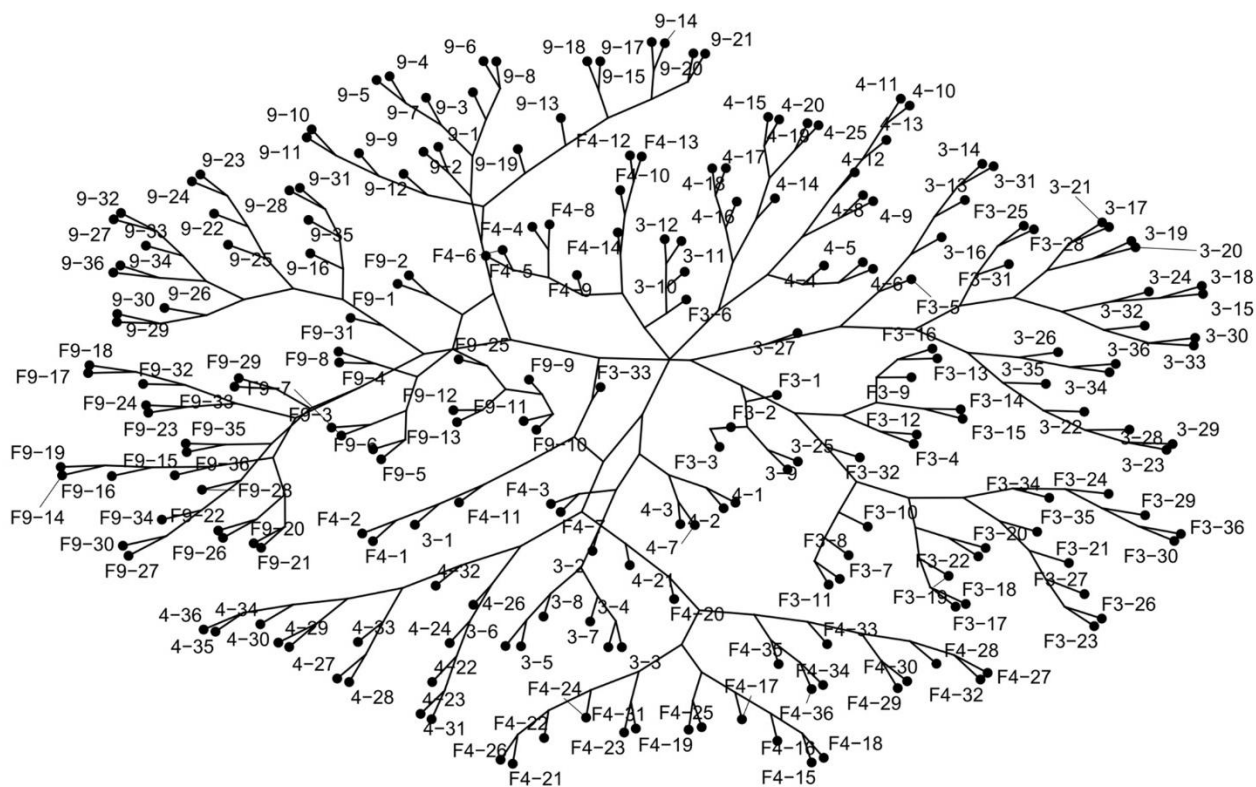
66

Figure S4. Visualization of the divisive hierarchical clustering of n-TiO$_2$ ⊂ sunscreen samples (samples 3, 4, and 9) before (X-Y) and after (FX-Y) exposure to fulvic acids where X and Y depict the sunscreen's ID and the number of replicates, respectively. F represents the exposure to fulvic acids.
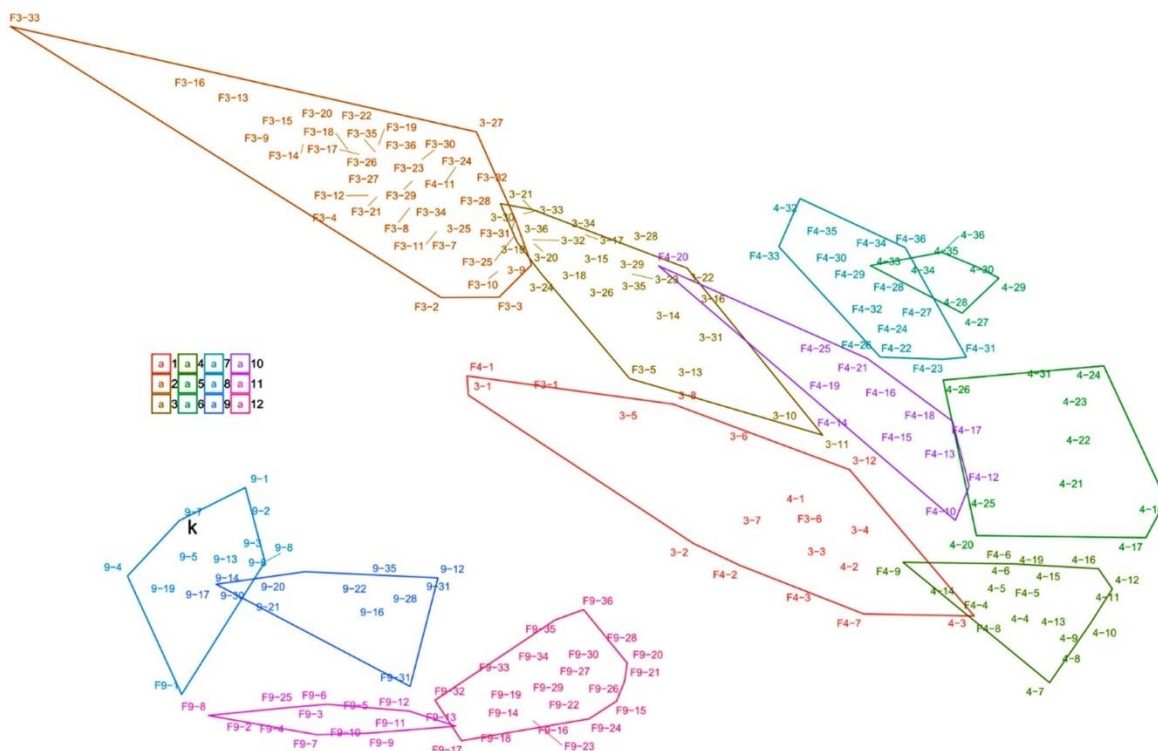
Figure S5. K-mean clustering of n-TiO$_2$ ⊂ sunscreen (samples 3, 4, and 9) before (X-Y) and after (FX-Y) exposure to fulvic acids where X and Y depict the sunscreen's ID and the number of replicates, respectively. F represents the samples exposed to fulvic acids. k depicts the optimized numbers of clusters. (Due to overlapping of the samples in 2D projection mode, not all the data points may be distinguishable).
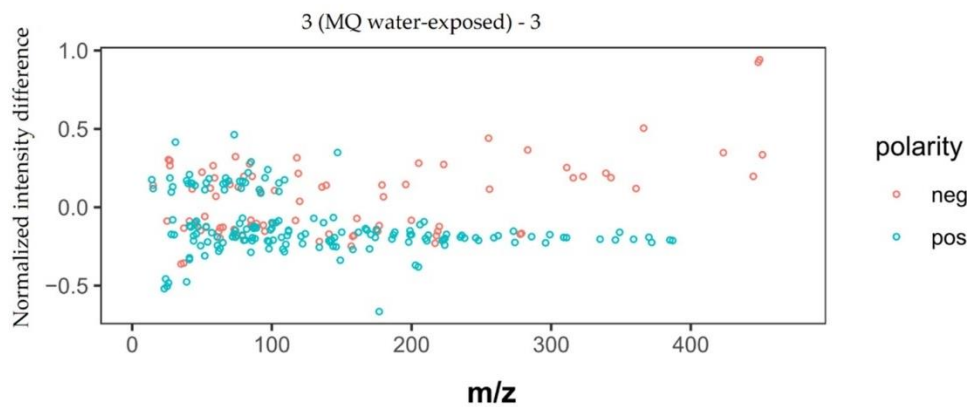

Figure S6. The intensity difference between 3 (MQ water-exposed)-3 where 3 (MQ water-exposed) is n-TiO$_2$ ⊂ sunscreen (3) exposed to pure water (instead of fulvic acids), and 3 depicts the initial n-TiO$_2$ ⊂ sunscreen (3). neg (red dots) depicts the negatively charged ions measured using ToF-SIMS, and pos (blue dots) depicts the positively charged ions measured using ToF-SIMS. MQ water is pure water.
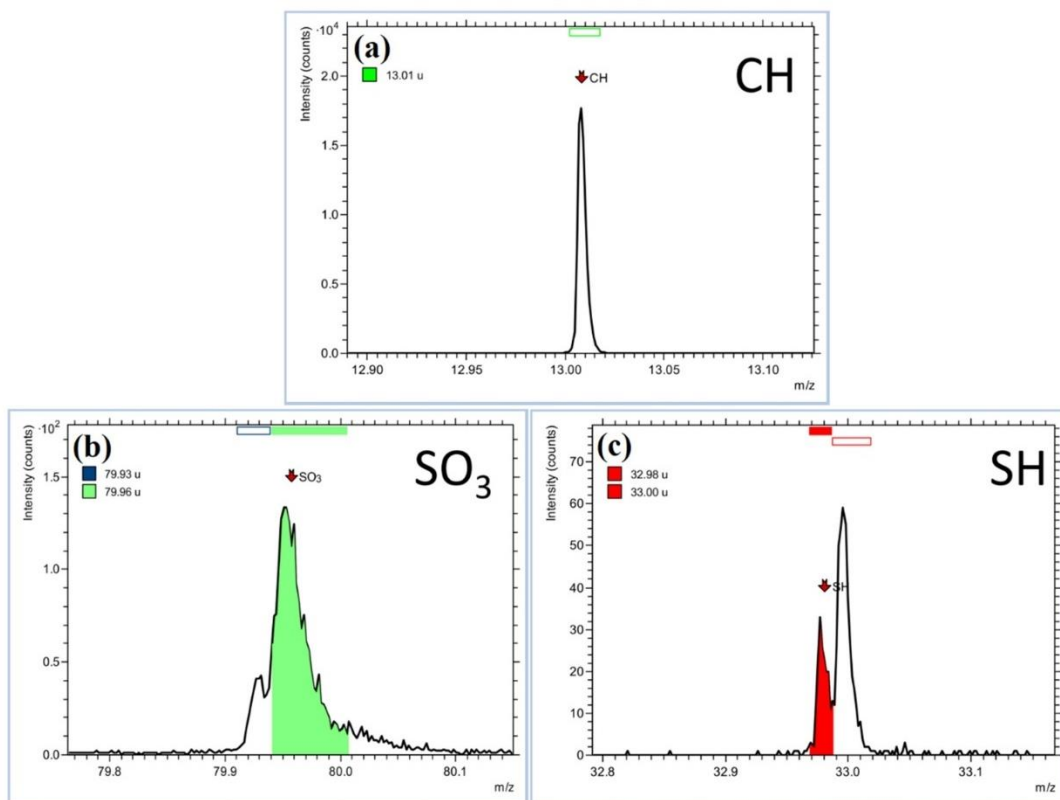
Figure S7. Mass (**a**) neg13.008 assigned to CH^-, (**b**) neg79.961 assigned SO_3^-, and (**c**) neg32.98 assigned to SH^- on the surface of n-$TiO_2 \subset$ sunscreen (3) exposed to fulvic acids.
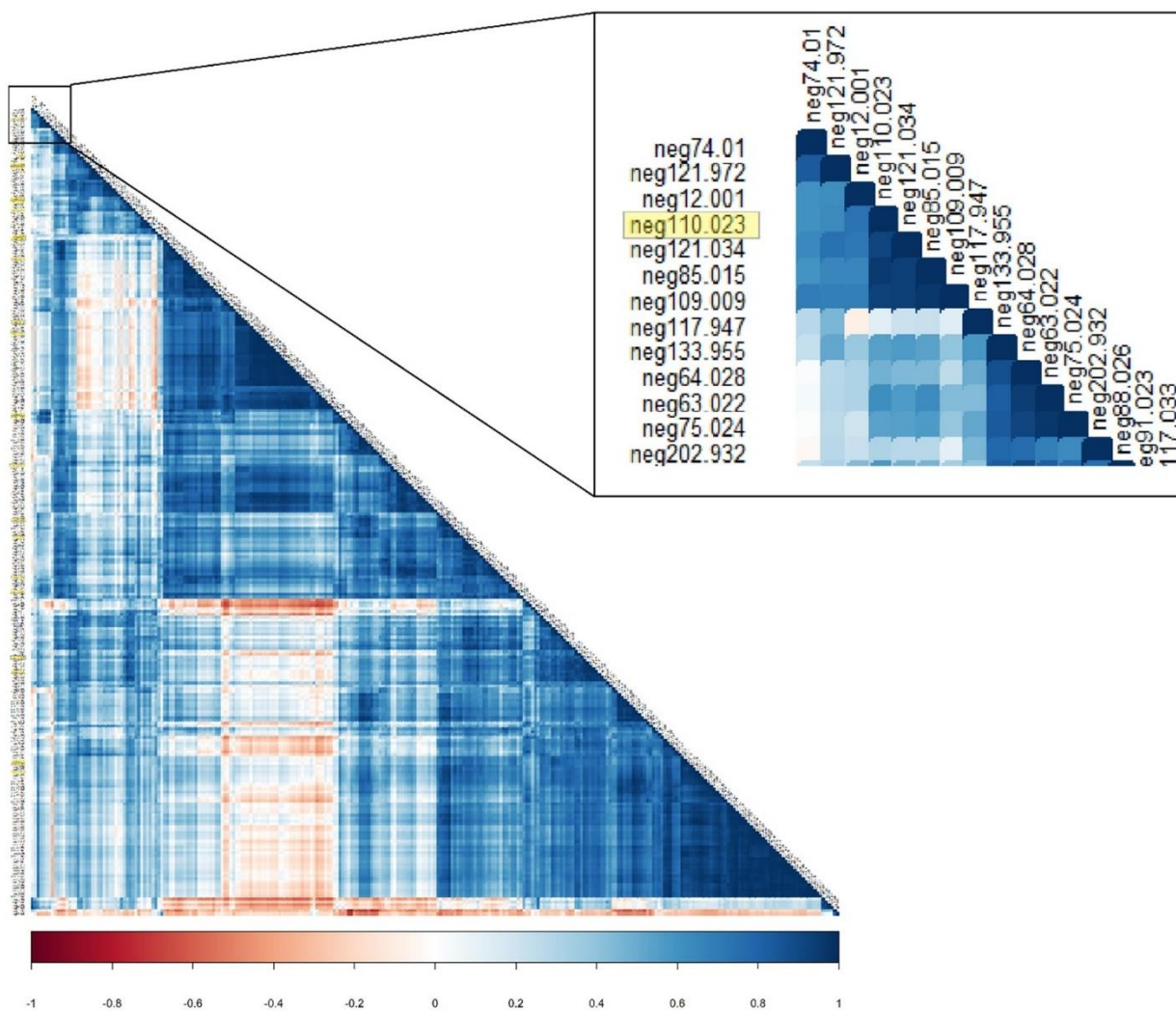
Figure S8. The correlation matrix of increased masses for sample F3 i.e. n-TiO$_2$ ⊂ sunscreen(3) exposed to fulvic acids. The variables are ordered using hierarchical clustering. Blue shows positive, and red shows negative correlations. The high-resolution image is available as a separate file on https://github.com/KunzstLD/Nanoparticle_classification.

8.7. Curriculum Vitae

Personal information:

Name:	Narjes Tayyebi Sabet Khomami
Nationality:	Iranian
Address (work)	Rheinland-Pfälzische Technische Universität (RPTU), Campus Landau, Fortstr.7, 76829 Landau
Email (work)	n.tayyebi@rptu.de

Education:

2017 - 2023	Ph.D., Natur- und Umweltwissenschaften, Rheinland-Pfälzische Technische Universität (RPTU), Campus Landau, Germany.
2011 - 2015	Ph.D., Inorganic Chemistry, Faculty of Science, Department of Chemistry, K. N. Toosi University of Technology, Tehran, Iran. GPA: 18.93/20
2008 - 2011	M.Sc., Inorganic Chemistry, Faculty of Chemistry, Kharazmi University, Tehran, Iran. GPA: 17.15/20
2003 - 2007	B.Sc., Applied Chemistry, Faculty of Chemistry, University of Tehran, Tehran, Iran. GPA: 15.67/20

Professional Experiences:

Doing an internship in a water and wastewater treatment plant in Tehran, 2007.

Instrument Proficiency:

FT-IR: The operator of FT-IR, K.N. Toosi University of Technology, Tehran, Iran, 2012-2014.

Fluorescence spectroscopy: Preparing and interpreting EEM data on surface water samples, University Koblenz-Landau, Landau, Germany, 2017-2023.

AFM: Analysing samples under air and fluid mode and interpreting the data, University Koblenz-Landau, Landau, Germany, 2022-2023.

Technical Skills and Languages:
MS Office
OriginLab
ChemLab
R (programming language)

Teaching Experience:
Teaching English, Tehran University, Tehran, Iran, 2008-2015.
Teaching Assistant (TA) for inorganic chemistry lab, K.N. Toosi University of Technology, Tehran, Iran, 2011-2015.
Instructor of General Chemistry for engineers, Azad University of Tehran, Tehran, Iran, 2012-2015.
Teaching environmental chemistry lab course, Koblenz-Landau University, Landau, Germany, 2017-2023.

Supervised Students:
Cynthia Precious Jusi (Master student, Koblenz-Landau University, Landau, Germany, 2019)
Parthvi Mayurbhai Patel (Master student, Koblenz-Landau University, Landau, Germany, 2020)

Projects:
Internano (DFG), Koblenz-Landau university, Landau, Germany, 2017-2021.
NaNaCo (DFG), Koblenz-Landau university, Landau, Germany, 2022-2024.

Peer-reviewed papers:

Tayyebi Sabet Khomami, Narjes, et al. "Sorption of Fulvic Acids onto Titanium Dioxide Nanoparticles Extracted from Commercial Sunscreens: ToF-SIMS and High-Dimensional Data Analysis." *Coatings* 12.3 (2022): 335.

Tayyebi Sabet Khomami, Narjes, et al. "Influential parameters of surface waters on the formation of coating on TiO_2 nanoparticles under natural conditions." *Environmental Science: Nano* 8.11 (2021): 3153-3166.

Tayyebi Sabet Khomami, Narjes, et al. "Validation of a field deployable reactor for in situ formation of NOM-engineered nanoparticle corona." *Environmental Science: Nano* 7.2 (2020): 486-500.

Tayyebi Sabet Khomami, Narjes, and Felora Heshmatpour. "Investigating the effect of immobilization of yttrium-Schiff base onto magnetite nanoparticles: enhanced catalytic activity in the synthesis of dihydropyrimidinones under solvent-free conditions." *Research on Chemical Intermediates* 42.3 (2016): 2087-2099.

Tayyebi Sabet Khomami, Narjes, and Felora Heshmatpour. "Magnetically recoverable nano-zirconium (IV) complex: enhancement of antibacterial activity." *Research on Chemical Intermediates* 43.2 (2017): 755-765.

Tayyebi Sabet Khomami, Narjes, F. Heshmatpour, and B. Neumüller. "A novel dinuclear zirconium (IV) complex derived from [Zr(acac)$_4$] and a pentadentate Schiff base ligand: Synthesis, characterization and catalytic performance in the synthesis of indole derivatives." *Inorganic Chemistry Communications* 41 (2014): 14-18.

Masteri-Farahani, M., and N. Tayyebi. "A new magnetically recoverable nanocatalyst for epoxidation of olefins." *Journal of Molecular Catalysis A: Chemical* 348.1-2 (2011): 83-87.

Book Chapter:

Masteri-Farahani, Majid; Tayyebi, Narjes (2015): Catalysis: Molybdenum-Based Hybrid Nanocatalysts. In: Kharisov, Boris Ildusovich; Kharissova, Oxana Vasilievna; Ortiz-Mendez, Ubaldo: CRC Concise Encyclopedia of Nanotechnology. Taylor & Francis. S. 100-114.

Selected Conference Presentations:

Validation of a field deployable reactor for in situ formation of NOM-engineered nanoparticle corona, 14th International Conference on Environmental Effects of Nanoparticles and Nanomaterials, 2019, Wien, Austria.

Influential parameters of surface waters on the formation of a coating on TiO_2 nanoparticles under natural conditions, 15th International Conference on Environmental Effects of Nanoparticles and Nanomaterials, 2022, Montreal, Canada (presented by Allan Philippe).